

PROGRESS: CAST MODULAR NODES FOR SEISMIC RESISTANT STEEL FRAMES

This interim report contains an update of the progress made on NSF CMS 01-96120 to the time period ending May 31, 2002. The report is organized according to connection concept: (A) Modular Connector; and, (B) Modular Node. A separate PDF file contains the results from this research.

Abstract

Modular connectors are being developed for use in seismic-resistant steel moment frames. The connectors are engineered specifically to meet performance requirements corresponding to optimal seismic response. The versatility in design required to accomplish this task is not readily available with traditional rolled shapes. Thus, the designs rely on advancements in materials and casting technology to create connectors specifically configured for seismic performance.

To date, three modular connection configurations have been developed: (1) a semi-rigid modular bolted connector for partially-restrained frames; (2) a cast modular node for moment-resisting frames; and, (3) a superelastic post-tensioned connecting system. Designs have been developed for each of the three configurations and an analytical program has been completed. The interim report focuses on the modular node and the modular connector.

Half-scale prototype specimens for the modular connector and full-scale prototype specimens for the modular node have been created. The experimental program testing the modular connector prototype has been performed; the modular node experimental program will commence in June 2002. The experiments exhibited excellent correlation with the analytical results. Improved seismic performance of the modular connector was confirmed through the experimental results.

A. Modular Semi-Rigid Connector For PRF's

Modular connectors are being developed for use in seismic-resistant steel moment frames. The connectors are engineered to meet performance requirements corresponding to optimal seismic response. The versatility in design required to accomplish this task is not readily available with traditional rolled shapes. Thus, the designs rely on advancements in casting technology to create connectors specifically configured for seismic performance.

A.1 INTRODUCTION

Modular connectors are being developed for use in seismic-resistant steel moment frames. The impetus for developing these connectors is the recently discovered susceptibility of steel special moment frames (SMFs) to fracture during earthquakes. These structures rely on the strength, stiffness and ductility provided by welded moment connections at the beam-to-column joints to create an efficient lateral-load resisting system [Popov et al, 1989]. However more than 100 SMFs suffered fracture at these welded joints during the Northridge [Malley, 1998] and Kobe earthquakes [Watanabe et al, 1998]. The poor performance of the welded moment connections has raised questions regarding the expected reliable ductility of these systems. This paper describes an attempt to find innovative solutions by combining aspects of modular construction and alternative

manufacturing processes.

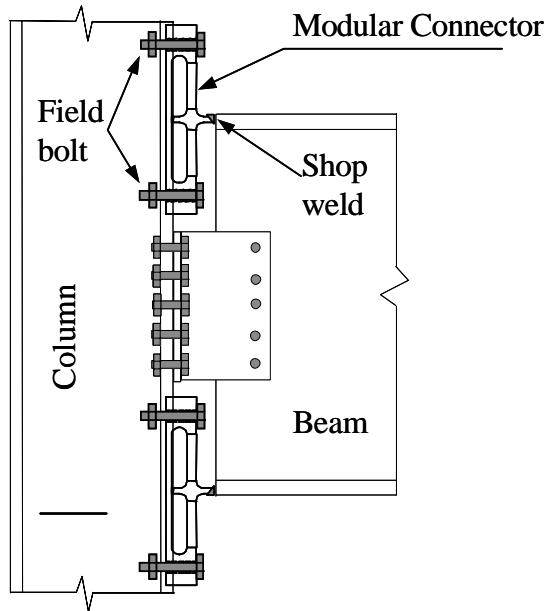


Figure 1. Location of Modular Connector.

A.1.a Modular Connector Concept

The modular connector (MC) is a cast piece used to connect the beam flange to the column. It is envisioned that typical construction will involve shop-welding the MC to beam flanges and field-bolting the MC to the column flange (See Figure 1).

The connectors possess a certain level of compliance, thus the joint will be, strictly speaking, semi-rigid. However, high rotational stiffness is achievable (See Section 5.B.2). In doing so, the MC provides a bolted alternative for full-moment connections that eliminates the potential for brittle behavior associated with welding construction. The MC concept is intended to provide reliable seismic performance for SMFs and offer improvements over traditional bolted connections. The MC is engineered to deliver reliable and repeatable energy dissipation through improved cyclic ductility. This objective is achieved through the elimination of concentrated plastic strain regions and the

reduction in bolt prying forces. The geometry required to produce such outcomes is not necessarily available in the configuration or fastening procedures associated with traditional rolled shapes. Thus, the MC will utilize the versatility afforded by casting processes to obtain optimal geometric configurations.

The MC is similar in form to the WT sections used in the traditional semi- or fully-rigid bolted connection, the tee-stub. However, the MC configuration contains major modifications that distinguish it from a tee-stub shape (see Figure 2). Foremost among these modifications are that: (1) The end regions of the connector are configured to reduce bolt force; (2) The principal flexural spans (arm elements) of the connector are transitioned into a variable cross-section piece to

reduce plastic strain demand. Each of these features is elaborated on below.

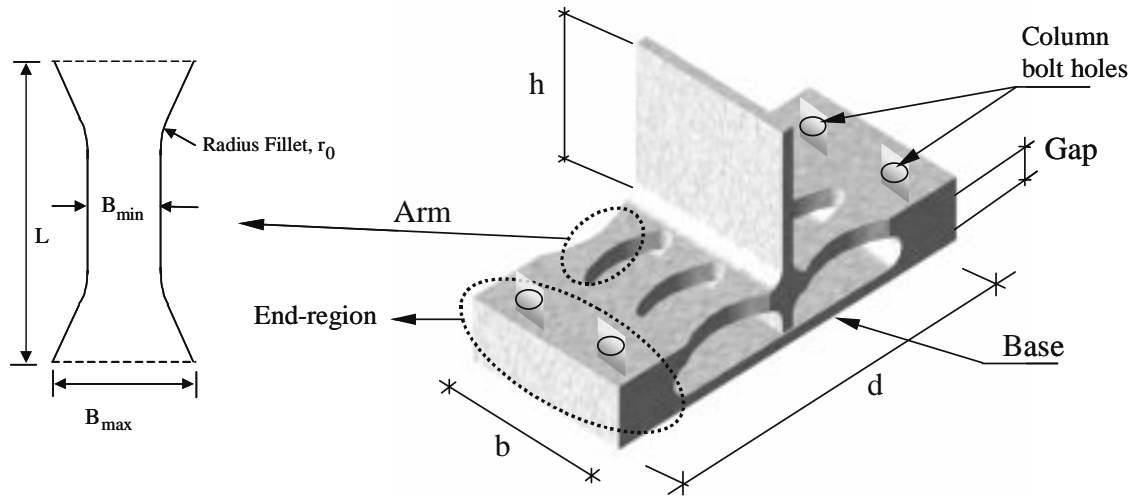


Figure 2. Typical configuration of modular connector.

(1) End-region configuration: The configuration of the end region is designed to reduce the prying forces that develop in the bolts under tension load. Reduction of force demands on the bolt is desirable from a capacity design standpoint as the bolt is less ductile than the mild steel detail pieces. The particular feature shown in Figure 2, the base configuration, is one of several end region configurations under investigation (See Sec. 3.A).

(2) Variable cross-section arm elements: The intent of the MC design is to develop the ductility within the connector itself. Therefore, the MC is detailed to dissipate energy through plastic deformation in the arm elements. These arm elements possess variable cross-sections to produce a plastic zone that is distributed along the entire length of the element. Such a distribution will reduce the intensity of strain concentrations that would occur, for instance, with the uniform section of the tee-stub shape. This approach has been used successfully in various metal dampers used primarily for bracing systems (See Sec. 2.A). However, certain differences exist in this application as will become apparent in the paper.

A.2 BACKGROUND

The MC concept under development is a modified version of a bolted semi-rigid connection, the tee-stub. The modifications employ concepts used in the development of a metal damper, the ADAS device. Readers unfamiliar with the ADAS device, or the mechanics of the tee-stub connection as it relates to seismic detailing, may find the following brief reviews instructive. Additionally, previous work performed by this research team on an alpha prototype is briefly summarized.

A.2.a X-Shaped Metal Dampers

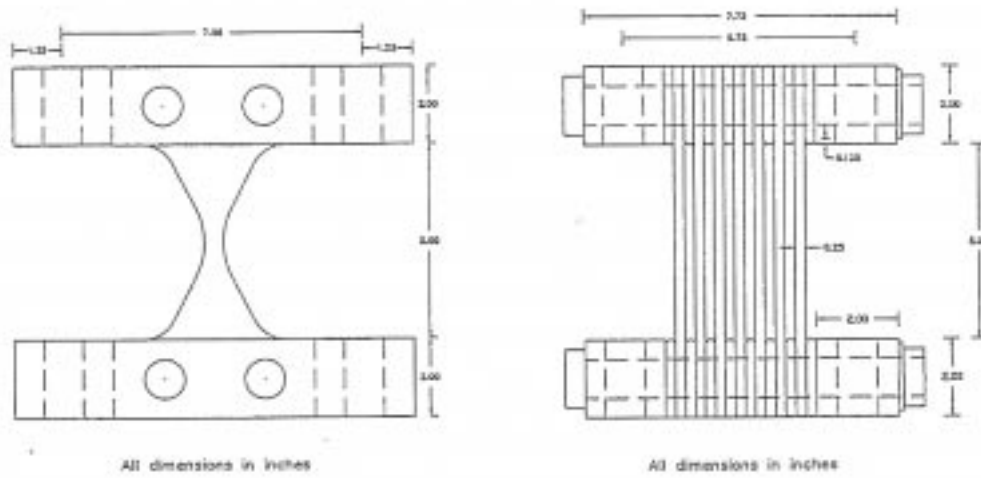


Figure 3. Added Damping and Stiffness (ADAS) Element

As a passive energy device, various metallic plate damper designs have been proposed over the past two decades. X-shaped plates were first developed as a piping support element and as an energy dissipating component of base isolation systems [Steimer, 1984]. More recently, researchers [Whitaker, Bertero et al., 1989] investigated the use of metal dampers to increase the dissipation capacity of conventional steel frames. These dampers, termed ADAS device (Added Damping and Stiffness Plate Elements), utilize an X-shaped profile in weak axis bending to efficiently spread the inelastic demand of reverse curvature flexural forces (See Figure 3a). In order to approach fixed-end boundaries, individual ADAS elements were bolted together at both ends (See Figure 3). Catenary forces were mitigated through compliance at the device ends in the modeling and configuring of the ADAS element. Accordingly, the effect of axial forces was neglected. Tests performed by Bergman (1987) and Whittaker (1989) showed that ADAS elements can safely be designed for displacement ranges up to about 10 times of yield displacement [Aiken et. al.].

The MC section follows an X-shape like the ADAS. In the MC application, catenary forces generate axial forces in the arms. Thus, the MC arms take on a different geometry than the ADAS as described subsequently.

A.2.b Bolted Tee-Stub Connections

Steel frames possessing bolted connections are being investigated as an alternative to perimeter welded moment frames [SAC, 1999] [Leon, 1999]. In a special moment frame (SMF) approach, the tee-stub is to remain elastic and energy dissipation is anticipated to occur in the beam. In a partially-restrained frame (PRF) approach, energy dissipation in the PRF is anticipated to occur within the semi-rigid connections. Figure 4 shows a common tee-stub detail piece. Typically, bolts are put as close to the fillet as possible (minimum gage), which provides maximum strength, maximum stiffness and minimum prying [LRFD, 1986]. However, minimizing gage dis-

tance results in high plastic strain demand. Used as an energy dissipater, concentrated hinges and prying forces develop in the tee-stub (See Fig. 5). The MC attempts to eliminate these behaviors as in the next section summarized.



Figure 4. Tee-stub detail.

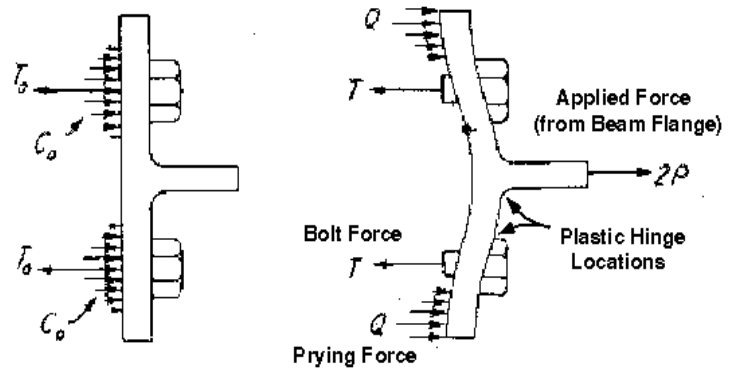


Figure 5. Prying forces on the tee-stub.

A.2.c Summary of Alpha Prototype Results

Cast forms have not been traditionally used as connections in building structure applications, thus little data exists for their use. An early version of the MC (alpha prototype) was investigated by previous researchers on this project. The alpha prototype resembles the current MC with the exception that the variable section is created through thickness reduction; termed an “hour-glass” arm. A base configuration was used for the end-region detail of the alpha prototype (See Figure 6).

Nonlinear finite element (FE) analyses and component experiments were performed to compare the response of the alpha prototype to a comparable tee-stub connection. The load versus displacement plot is shown for the alpha prototype and the analogous tee-stub (See Figure 7). This plot indicates that the alpha prototype and tee-stub are nominally similar in stiffness and strength; however the alpha prototype does achieve greater overstrength. This overstrength is due to signifi-

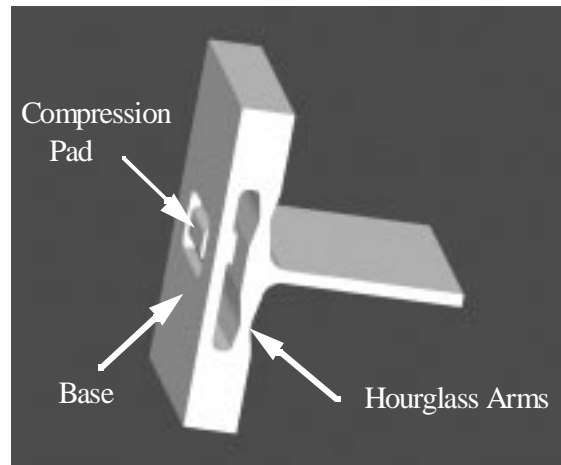


Figure 6. Alpha Prototype.

icant catenary action produced by the presence of the base (See Sec. 5.B.6)

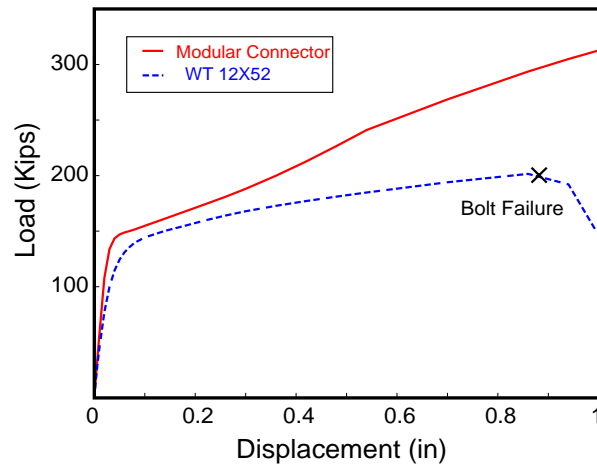


Figure 7. Load-Displacement Comparison

Figure 8 shows half-symmetry models of the tee-stub detail piece and a modular connector of similar strength and stiffness. Equivalent plastic strain is shown in the contours at the identical deformation demand (0.033 rad for W30 beam). Hysteretic energy dissipation is achieved in the tee-stub piece through concentrated plastic hinges adjacent to the bolt head and the outstanding leg (See Fig. 8b). Conversely, the plastic zone in the hourglass arms is spread (See Figure 8a).

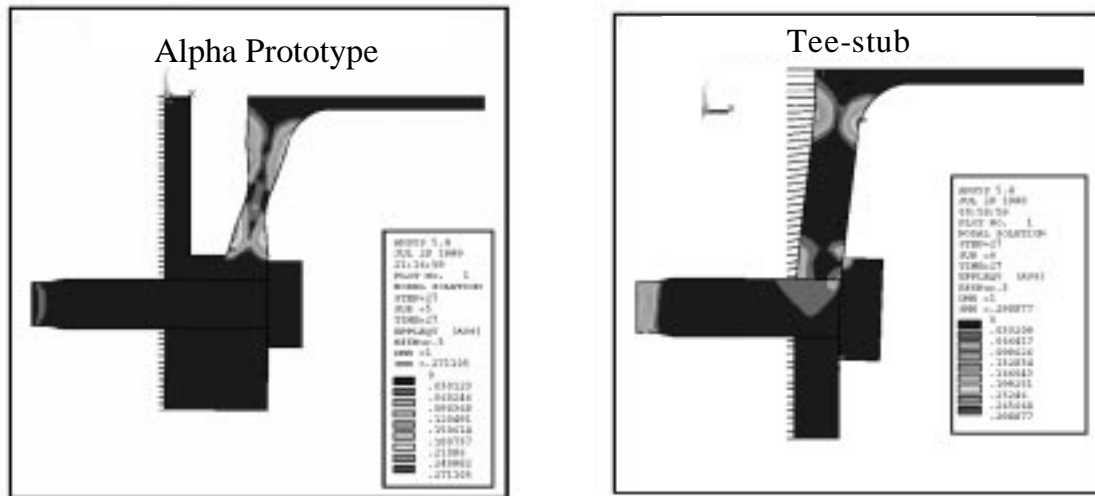


Figure 8. Plastic Strain Demand Comparison: (a) Alpha Prototype; (b) Tee-stub.

The end region reduces demand on the bolt. Accordingly, the alpha prototype exhibits: (1) significantly lower plastic strain in the bolt threads; (2) no plastic behavior in the bolt shank, lower plastic strain in the detail piece in comparison to the tee-stub.

Indicated in Figure 9, the point of bolt thread failure [Kulak et al, 1987] occurs earlier in the tee-stub. Figure 10 shows the significant reduction in prying forces in the alpha prototype with

respect to the tee of similar strength and stiffness. Note that the bolt pretension in the alpha prototype is overcome at about twice the applied load.

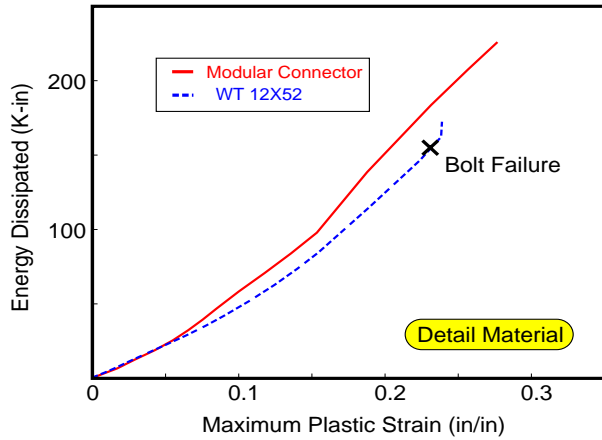


Figure 9. Connector Plastic Strain

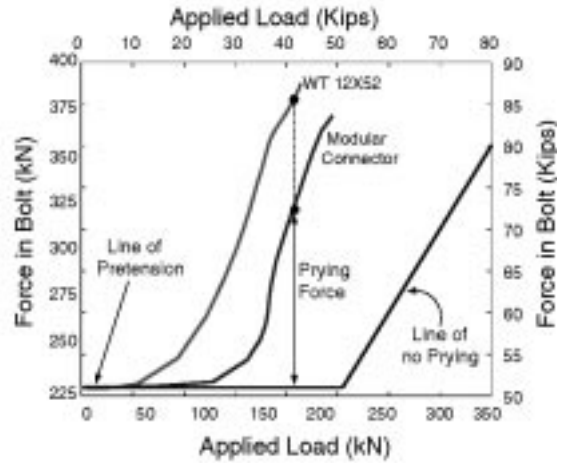


Figure 10. Comparison of Prying Action

A cyclic test of the alpha prototype was performed. The casting was cycled 13 times at 0.4” prior to a low-cycle fatigue (LCF) failure (See Figure 11). The analytical curve shown in the figure indicates that the FE results estimate the strength accurately but overestimate the initial stiffness. The LCF failure of the alpha prototype occurred in the high tensile stress region of the alpha prototype arm (See Figure 12). This region contains high tension due to combined flexure and catenary action in the arm. The alpha prototype experimental results did not show significant improvement in ductility over tests of the tee-stub connection. Therefore, the design was modified to the current (beta) MC prototype as described in the main body of this paper.

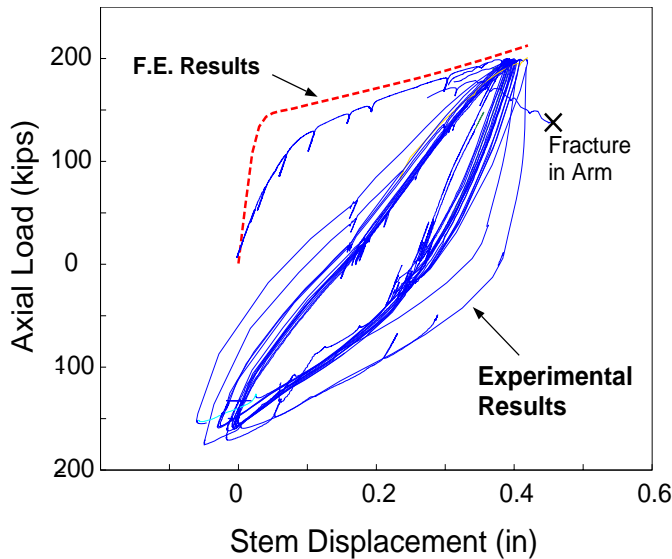


Figure 11. Hysteresis Curve: Alpha Prototype Experiment



Figure 12. Fracture of alpha prototype

A.3 DEVELOPMENT OF MC PROTOTYPE

The development of the modular connector (MC) is driven by a comprehensive analytical and experimental program. The objectives of the analytical program are to: (1) determine the effects of different end-region conditions for the MC and select the most promising configuration; (2) determine the optimal shape of the MC arm region; and, (3) provide a prediction of the behavior of the MC prototype for determining required experimental capabilities. This section describes the steps taken to meet the first two objectives. The description of the step to accomplish the final objective accompanies the section of experimental verification of the prototype MC.

A.3.a End-Region Alternatives

The primary intent of the end-region design is to minimize the high prying forces and moments that would otherwise occur in bolts at longer gages. The end-region also provides a stiff boundary for the arms. Four end-region configurations termed MC-Base, MC-NoBase, MC-Outrigger, and MC-Eccentric are examined (See Figure 13).

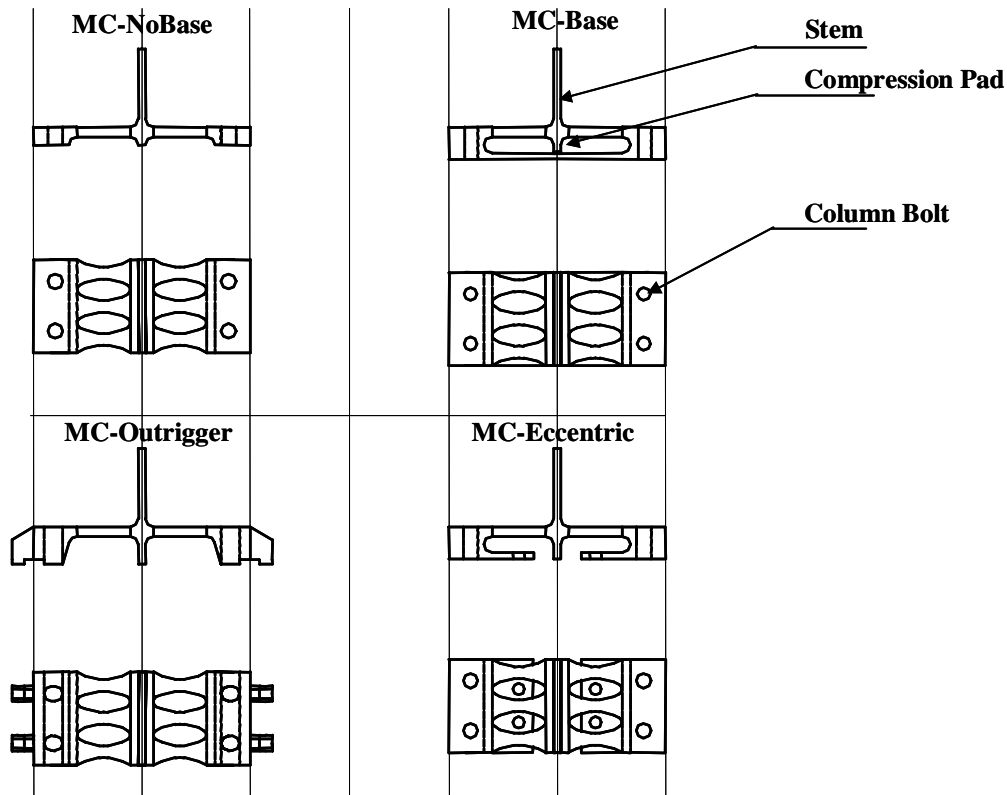


Figure 13. Possible end-region configurations

The MC-Base end region configuration contains a back piece or base which connects each end region. The base significantly reduces prying forces and additionally provides a near fixed boundary for flexure of the arms. The MC-eccentric configuration has an end-region which contains secondary bolts eccentric to the main bolts. These secondary bolts decrease the rotation of the end-region. The MC-outrigger configuration employs an extending outer bearing pad which

increases the leverage of the contact region. The outrigger thus decreases the prying forces and moments. The MC configuration without the base is used as a control to compare the MC directly to a WT, thus allowing the effects of the base and the arms to be isolated.

Note that for each configuration an element at the junction of the arms protrudes to the back of the connector. This feature, termed a compression pad, is provided to transmit the beam flange compressive loads directly to the column as the MC cycles between tension and compression loading during seismic response. This feature is necessary to reduce pinching of the hysteresis curves and to greatly reduce the strain demand in the connector arm.

A.3.b Arm Geometry

The arm geometry is described by four main geometric parameters as indicated in Figure 14: (a) maximum width, B_{max} , at the end of the arm; (b) minimum width, B_{min} , at the middle of the arm; (c) length of the arm, L ; and, (d) arm thickness, t . The variable section follows an X-shape, as shown with the dotted line, until the minimum width is reached. A transition fillet occurs at this point.

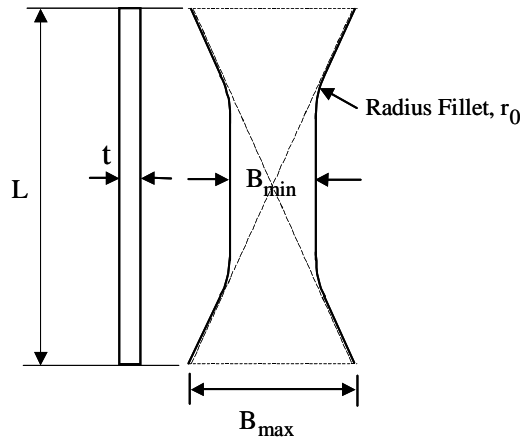


Figure 14. Hourglass Arm in MC

An extensive parametric study was performed to obtain the optimal geometry of the MC arm. The following relationships of arm dimensions were used as critical ratios:

- (a) Width reduction ratio (B_{min}/B_{max})
- (b) Length to width ratio (L/B_{max})
- (c) Fillet radius (with respect to arm length) (r_0/L)

B_{min} , B_{max} , L , r_0 , and t were varied to investigate the optimum geometry ratios. Table 1 provides the complete description of the parametric study. Geometry efficiency was examined in three ways: (1) L was varied while keeping B_{min}/B_{max} constant, (2) B_{min} was varied while keeping L/B_{max} constant, (3) r_0 was varied while keeping B_{min}/B_{max} and L/B_{max} constant. Arm thicknesses were selected to meet the strength capacity and stiffness required of the connector. An arm of constant width and thickness serves as the control.

The BMIN series investigates the effect of varying the minimum width for given arm length and maximum width. The LB series examines varying length to width ratio while keeping the width reduction ratio constant. In the LT series, the thickness was varied for optimum

B_{min}/B_{max} , L/B_{max} and r_0 . The T series investigates the effect of thickness for various width reduction ratios. The Ω series examines the effect of geometric ratios and thicknesses to the overstrength ratio (See Section 5.B.6).

Table 1: Parametric study of the arm geometry

Study ID	# of runs	L (in)	B_{min} (in)	B_{max} (in)	r_0 (in)	t (in)	$\frac{B_{min}}{B_{max}}$	$\frac{L}{B_{max}}$
BMIN1	7	3	0.6 ~ 0.9	1.5	2.5 ~ 3.3	0.75	0.4 ~ 0.6	2
BMIN2	6	4	0.6 ~ 1.2	2	2.5	0.75	0.3 ~ 0.6	2
BMIN3	5	5	0.75 ~ 1.5	2.5	2	0.75	0.3 ~ 0.6	2
LB1	8	3	0.5 ~ 3	1 ~ 6	3.15 ~ 1.2	0.75	0.5	0.5 ~ 3
LB2	8	4	0.5 ~ 4	1 ~ 8	2 ~ 1.6	0.75	0.5	0.5 ~ 4
LB3	7	5	0.75 ~ 5	1.5 ~ 10	2	0.75	0.5	0.5 ~ 3.3
Ω 1	5	5	1.25	1.5	2	0.5 ~ 2.5	0.5	2
Ω 2	3	5	2.5 ~ 7	5 ~ 14	2 ~ 1.75	1	0.5	0.36 ~ 1
Ω 3	3	7	1.75	3.5	2	1 ~ 3	0.5	2
T	4	4	0.6 ~ 1.3	2	2	1	0.3 ~ 0.65	2
LT1	4	3	0.675	1.5	2.8	0.5 ~ 1.5	0.45	2
LT2	4	4	0.9	2	2.5	0.5 ~ 1.5	0.45	2
LT3	4	5	1.125	2.5	2	0.5 ~ 1.5	0.45	2
LT4	2	6	1.35	3	2	1, 2	0.45	2
Stretch1	3	3, 4, 5	0.675	1.5	2.8	0.75	0.45	2 ~ 3.33
Stretch2	3	3, 4, 5	0.9	2	2.2	0.75	0.45	1.5 ~ 2.5
Stretch3	3	3, 4, 5	1.125	2.5	1.85	0.75	0.45	1.2 ~ 2

A.4 ANALYTICAL MODELING

The analytical program for development of the modular connector involved two separate investigations: (A) Evaluation of end-regions; and, (B) Evaluation of the arm geometry. The modeling for each is described in the following.

A.4.a End-Region Evaluation: 2D Model

In order to rapidly evaluate several end region configurations for the MC, a 2D model was used to represent a tributary cross-section of the MC. The 2D MC model is a plane-stress representation of a single arm of the MC with a scaled representation of the column bolt (for instance the MC in Fig. 13 has three arms and two column bolts, thus the model contains one arm and 2/3 of the column bolt). Plane-stress quadrilateral solid elements model the angle; plane-stress quadrilateral solid elements model the bolt; point-to-point pseudo-elements capture contact between the MC, bolt and column flange. The load is applied in displacement control at the MC stem. 40ksi material is used in end-region FE analysis.

The validity of this approach, including boundary effects and appropriate mesh refinement

was established in the alpha prototype research [Hoskisson, MS Thesis, 2000]. The variation in configuration required in the modeling was facilitated by the parametric design language and adaptive meshing features of the commercial software ANSYS. Figure 15 shows the 2D FE model in half-symmetry representation about the stem.

The model includes material and geometric nonlinearity, the latter due to changing contact surface and catenary action at large deflection. Thus, the element constitutive relationships utilize material plasticity and large deformation capabilities. The distributed plasticity formulation inherent in the solid model is instrumental in capturing shear and shear/flexure modes present in the MC. The material model employs multi-linear kinematic hardening principles, the Von Mises yield function, and the Prandtl-Reuss Flow Equation (ANSYS Theory). Mild steel stress-strain curves are reproduced from uniaxial tension tests for the cast steel and converted into true stress/logarithmic strain for large deformation analysis. The stress-strain curve is represented by a detailed piecewise-linear relationship in order to accurately capture the high strain gradients within the plastic zones.

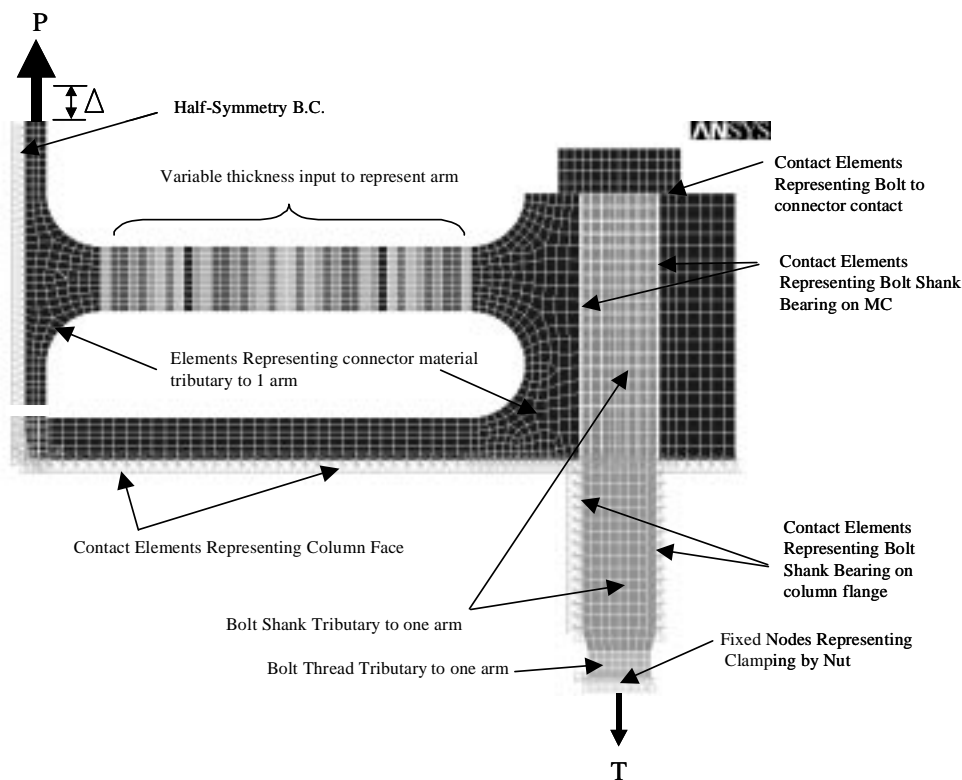


Figure 15. Two-dimensional FE model of MC.

The elements modeling the bolt use a plane-stress formulation equivalent to the area of the bolt tributary to one arm of MC. The aspects of bolt behavior captured in the model include preload, slip, bearing, axial/rotational flexibility, non-uniform pressure distributions, and fastener inelasticity. The nominal geometry of the shank region is preserved in the elements representing the bolt; the geometry of the thread region and material model is calibrated to match yield load, yield deflection and secondary stiffness from uniaxial test data of individual fasteners. Fixed sup-

port models the restraint of the nut, thus providing a reasonable representation of the flexural rigidity provided by the bolt. A coefficient of friction of 0.5 is used, based on empirical observation. The bolt pretension is developed by applying an initial interference to the angle-bolt head interface using an equilibrium step. An initial gap between the bolt shank elements and the adjacent angle elements corresponding to one-half the standard bolt hole tolerance (1/32”) allows realistic bearing response following bolt slip.

A.4.b MC Arm Shape Evaluation: 3D Model

A fine-mesh three dimensional (3D) nonlinear finite element model was used to evaluate the MC arm shape. The model is comprised of eight-noded solid elements with large deformation capability

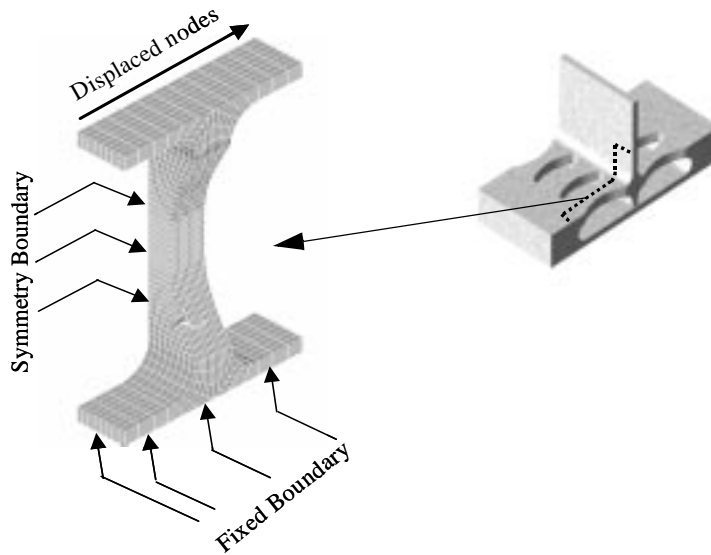


Figure 16. Half-symmetry FE model of MC arm

The region encompassed by a model is the half symmetry representation of a single arm (See Figure 16). A small region of the MC body is also modeled at either end to produce a realistic boundary condition at the arm terminus. Bottom nodes are fixed and the top nodes are displaced about the weak axis of bending. *In 3D FE models, 50ksi material is used.*

A.4.c Performance Criteria

The equivalent plastic strain is defined as:

$$\epsilon_{pl} = \frac{1}{1+\nu} \left(\frac{1}{2} [(\epsilon_1 - \epsilon_2)^2 + (\epsilon_2 - \epsilon_3)^2 + (\epsilon_1 - \epsilon_3)^2] \right)^{1/2} \quad (1)$$

$\epsilon_1, \epsilon_2, \epsilon_3$ are the principal total strains and ν is the effective plastic poisson's ratio (0.5) [ANSYS theory manual].

The prying force can be formulated as (See Figure 5 and 10):

$$F_p = T \mathfrak{D} \max(P, PT) \quad (2)$$

F_p is the prying force, T is the bolt force, P is the applied load, PT is the pretension force in the bolt.

The following quantities were measured in the analyses and used as performance criteria for comparison between the MC and the tee-stub. (see Figure 17):

- overall load-displacement of the stem ($P-\Delta$)
- maximum equivalent plastic strain in bolt head (ϵ_{hd}^{pl}), bolt shank (ϵ_{sh}^{pl}), bolt threads (ϵ_{th}^{pl}), and MC arm (ϵ_{arm}^{pl})
- bolt head moment (M_{hd}) and rotation (θ_{hd}) at bolt head
- bolt force (T) and prying force (F)

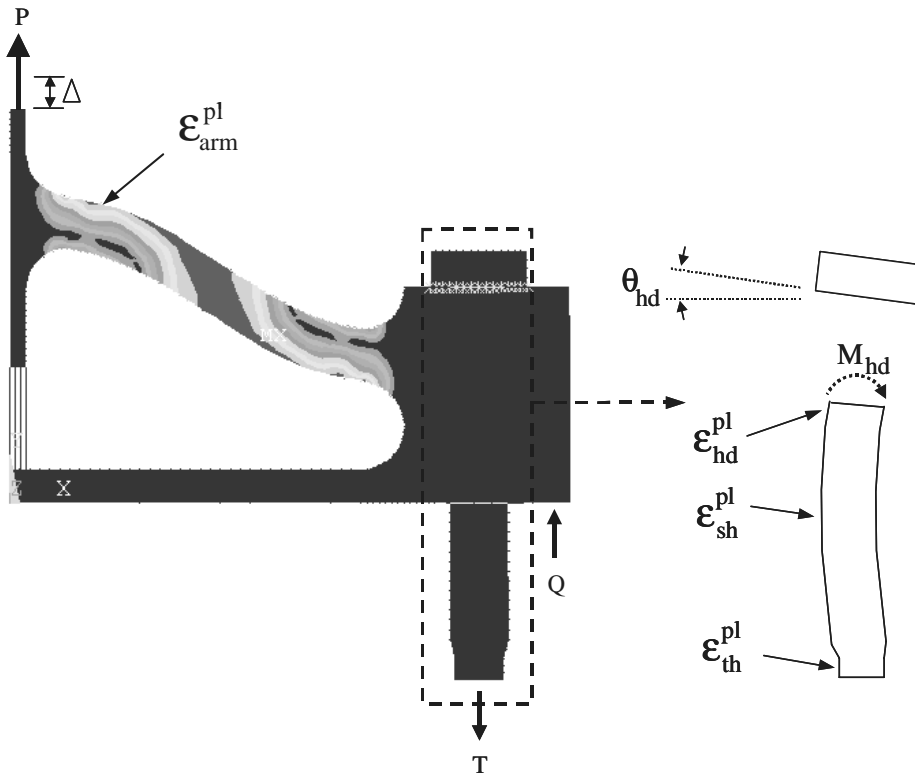


Figure 17. Performance criteria for connector comparisons

In order to represent rotation values in translational analysis, a 30" beam depth was assumed. A connector deforms at 1.5" represents a 0.05 rad rotation.

For consistency in comparisons, three strength definitions are used:

(1) Yield strength (P_y) is defined as the strength of the MC when outer fibers of the MC arm yields. The yield strength can be approximated using classical methods as follows:

$$P_y = 2 \left(\frac{M_p}{L} \right) \quad (3)$$

substituting the geometric parameters of the MC arm results in

$$P_y = n \left(\frac{2 \left[\left(\frac{1}{4} B_{max} t^2 \right) (F_y) \right]}{L} \right) \quad (4)$$

rearranging the equation 4 and using the optimum L/B_{max} result in,

$$P_y = \frac{n(F_y)t^2}{2 \left[\frac{L}{B_{max}} \right]_{optimum}} \quad (5)$$

where, n is the number of MC arms; F_y is the yield stress.

(2) A “useable” strength ($P_{0.05}$) defined as the strength of the MC at 0.05rad rotation.

(3) The actual ultimate strength of the MC is termed the stability point (P_u).

The overstrength ratio of the load deflection curve at the stability point (Ω_u) is defined as the ratio of P_u to P_y . Similarly, overstrength ratio at 0.05rad ($\Omega_{0.05}$) is the ratio of useable strength to P_y (See Figure 18).

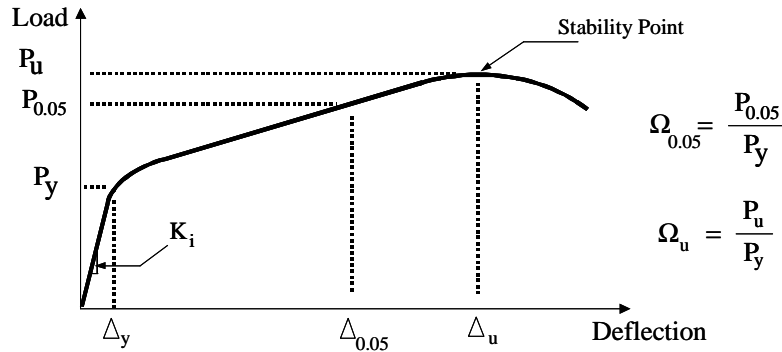


Figure 18. Typical load deflection plot and overstrength formulation of the MC.

The MC arm is assumed to be failed when the maximum equivalent plastic strain demand

reaches 0.285. This demand is defined as critical equivalent strain for the MC arm. Similarly, the column bolt is assumed to be failed when the maximum equivalent plastic strain reaches 0.06. Ductility of the MC arm is defined as the ratio of the equivalent plastic strain demand to the critical equivalent strain.

Minimum crosssectional area of the MC arm is defined as critical area (A_{crit}) and is formulated as follows:

$$A_{crit} = B_{min}(t) \quad (6)$$

The alpha index is defined as the ratio of the maximum equivalent plastic strain in the MC arm to the yield strength of per unit width of the MC arm.

$$\alpha = \frac{\epsilon_{arm}^{pl}}{P_y/B_{min}} \quad (7)$$

The useable life of the MC is governed by one of the following: (1) low-cycle fatigue created by cyclic plastic strain at one of the plastic hinge regions in the MC arm; (2) exceedance of the plastic strain capacity due to successive axial load increments in the bolt threads; or, (3) cyclic plastic strain demand due to flexure of the bolt shank.

A.5 PROTOTYPE DEVELOPMENT AND EXPERIMENTAL PROGRAM

Experimental program consisted of two stages (A) pilot tests; (B) full-scale beam-column tests to be tested individually under cyclic and monotonic loads. Only the pilot tests are addresses in this report.

By testing individual MCs instead of entire beam-column subassemblages, a large number of parameters was investigated economically and rapidly. In Figure 19 and Figure 20, typical pilot IMC-Base and MC-NoBase prototypes are shown.



Figure 19. MC-Base



Figure 20. MC-NoBase

The typical pilot MC configuration and arm dimensions are shown in Figure 23 and 24 respectively.

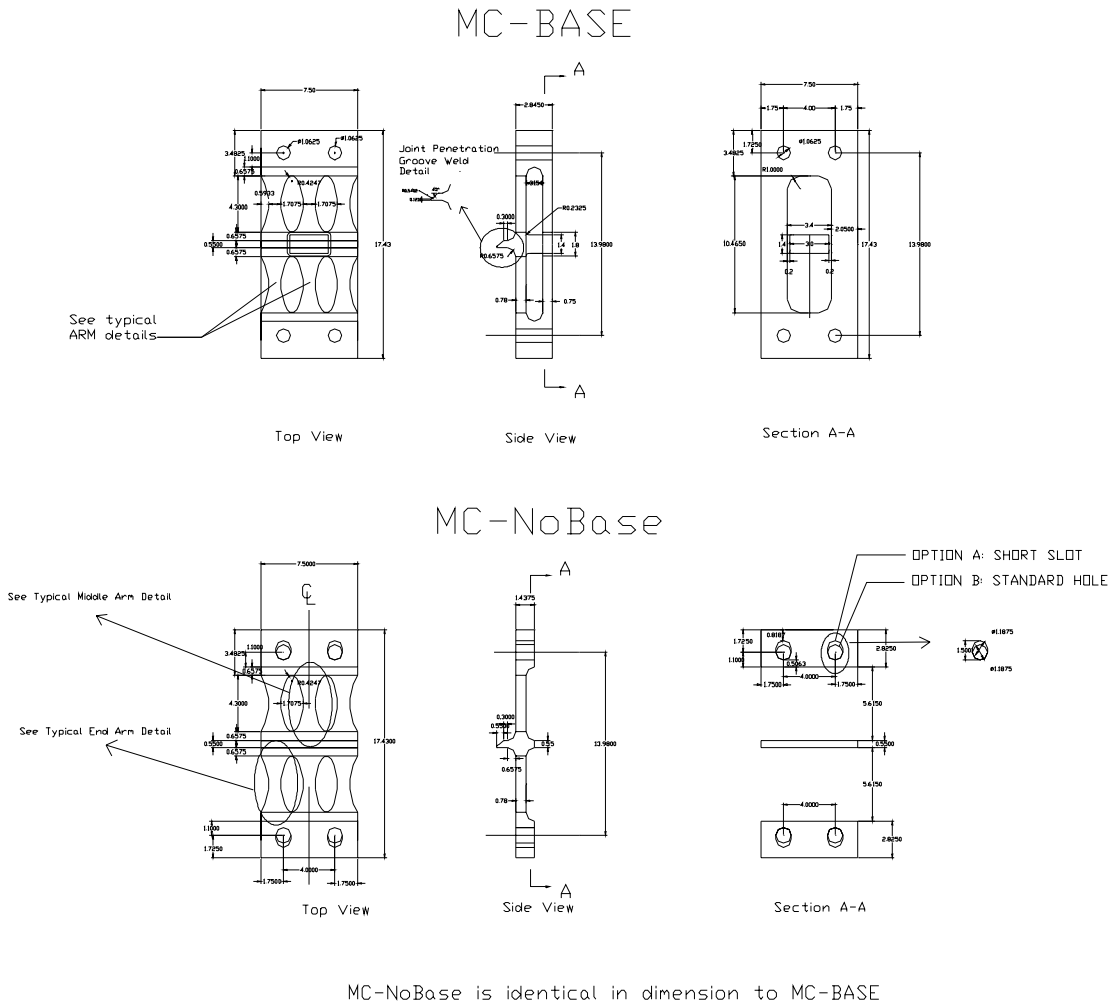
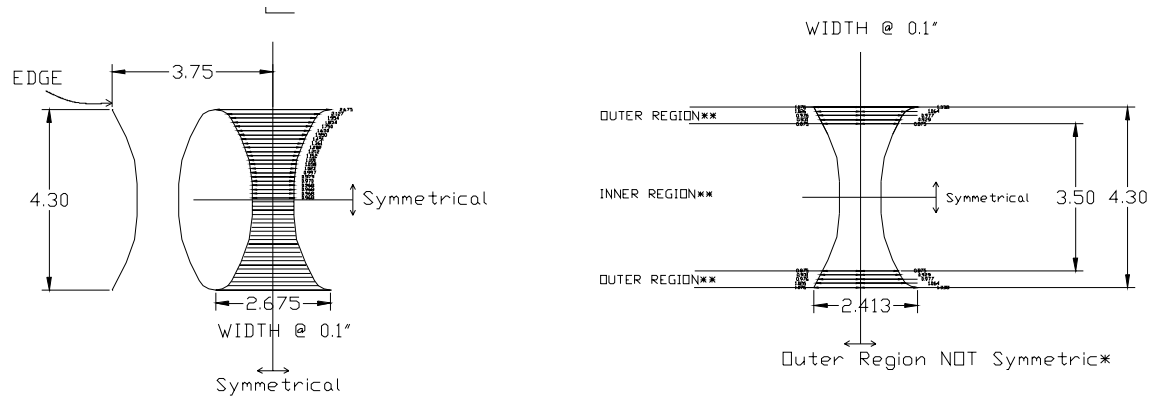


Figure 23. Typical MC-Base and MC-NoBase dimensions.



Typical Middle Arm Detail

Typical End Arm Detail

Figure 24. Typical MC arm detail.

Table 2 summarizes critical dimensions and ratios of the pilot MC arm. Material properties for the entire pilot test program are shown in Table 3.

Table 2: MC Arm properties

Test ID	L (in)	B _{min} (in)	B _{max} (in)	t (in)	L / B _{max}	B _{min} / B _{max}
MC-Base and MC-NoBase	4.3	0.968	2.15	0.78	2	0.45

Table 3: Material properties

Series	Mill F _y (ksi)	Mill F _u (ksi)	Mill Elongation (%)
MC-Base	43	67.6	32
MC-NoBase	48.4	69.4	31.5

The connectors were subjected to axial loads in order to represent the beam flange forces in actual connections. The axial loading is a simplification of the actual conditions, shear forces present in the actual connection were missing in the pilot tests. One MC-Base was tested monotonically to provide reference points for comparing the cyclic data. The cyclic load history specified in the FEMA-350 testing protocol was used. It consisted of several steps of the increasing rotations, each made up of several cycles. A system of force and displacement limits was used for the cyclic tests. During the tension portion of the first cycle of a given step, the stem of the connector was pulled to a given displacement and then pushed back in to the initial position. The connector was then

pushed in compression until a load approximately equal to the tensile load was reached. This system of force and displacement limits was used for all of the cyclic tests.

Table 4: Pilot Test and Full Scale Test Descriptions

Series	Test ID	Type of Loading	Bolt Designation	Notes	Status
MC-Base	Mono-Base-1	Monotonic	1" - A325	Without guide plates	Completed
	Cyc-Base-1	Cyclic	1" - A325	Without guide plates	Completed
	Cyc-Base-2	Cyclic	1" - A325	With guide plates	Completed
	Cyc-Base-3	Cyclic	1" - A325	With guide plates	Completed
	Mono-Base-1	Monotonic	1" - A325	Without guide plates	in progress
	Cyc-Base-4	Cyclic	1" - A325	With guide plates	in progress
MC-NoBase	Mono-NoBase-1	Monotonic	1 $\frac{1}{8}$ " - A490		Completed
	Cyc-NoBase-1	Cyclic	1 $\frac{1}{8}$ " - A490		Completed
	Mono-NoBase-2	Monotonic	1" - A325		in progress
	Cyc-NoBase-2	Cyclic	1" - A325		in progress
Tee-Stub	Mono-WT-1	Monotonic	1" - A325	Standard Slot	in progress
	Mono-WT-2	Monotonic	1" - A325	Short Slot	in progress
	Mono-WT-3	Monotonic	1 $\frac{1}{8}$ " - A490	Standard Slot	in progress
	Mono-WT-4	Monotonic	1 $\frac{1}{8}$ " - A490	Short Slot	in progress
	Cyc-WT-1	Cyclic	1" - A325	Standard Slot	in progress
	Cyc-WT-2	Cyclic	1" - A325	Short Slot	in progress
	Cyc-WT-3	Cyclic	1 $\frac{1}{8}$ " - A490	Standard Slot	in progress
	Cyc-WT-4	Cyclic	1 $\frac{1}{8}$ " - A490	Short Slot	in progress
Full Prototype	Mono-Full-1	Monotonic	1 $\frac{1}{8}$ " - A490		in progress
	Cyc-Full-2	Cyclic	1 $\frac{1}{8}$ " - A490		in progress
	Cyc-Full-3	Cyclic	1 $\frac{1}{8}$ " - A490		in progress
	Cyc-Full-4	Cyclic	1 $\frac{1}{8}$ " - A490		in progress

Pilot testing was conducted using a specially designed and constructed fixtures. The stem and end-regions of the MC were bolted to the stiffened fixtures that were in turn connected to 220 kip actuator (See Fig. 25 and 26).



Figure 25. Bottom fixture for MC pilot testing

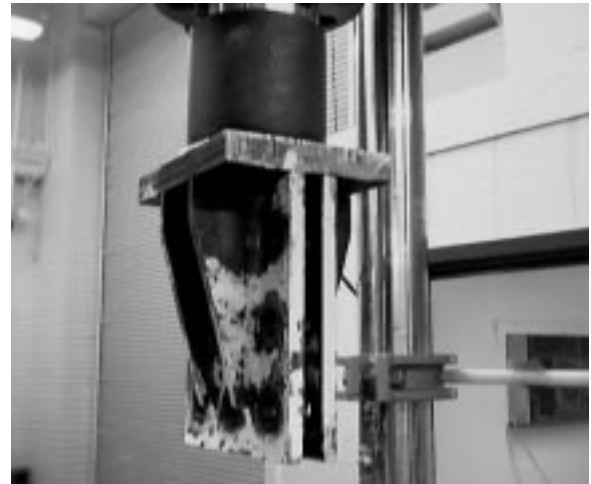


Figure 26. Top stiffened fixture for MC pilot testing

Figure 27 shows the MC-Base prior to loading. In Figure 28, the instrumentation layout is shown. Linear variable displacement transformers (LVDTs) were used in order to measure the deformation components in different locations. LVDT I measured the overall deflection, II and III measured deflections at the end-region in order to calculate the end-region rotation and connector slip, IV and V measured the displacement at bolt head in order to calculate the bolt rotation, VI measured the bolt slip. VII indicates the use of bolts instrumented with strain gauges to monitor bolt forces, including the bolt moment. VIII indicates the use of MC arms instrumented with strain gauges to monitor the strain demands. Similarly, strain gages at the base to monitor the base forces is indicated by IX. Figure 29 shows the strain gauge layout on the MC arm. 5 strain gauges each for the top and bottom surface of MC arm were put in order to measure strains up to 20%. Location A, B, D and E indicates high flexure region, C indicates necking region.

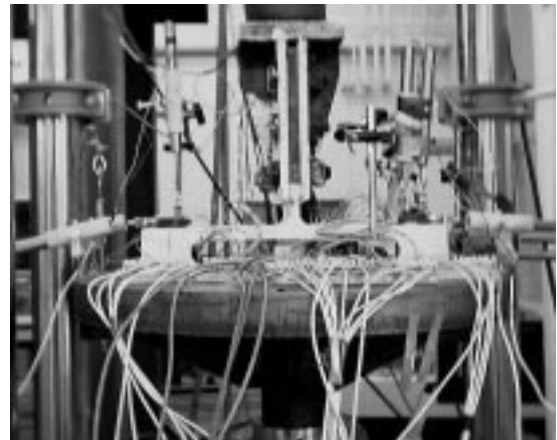


Figure 27. MC-Base in testing fixture

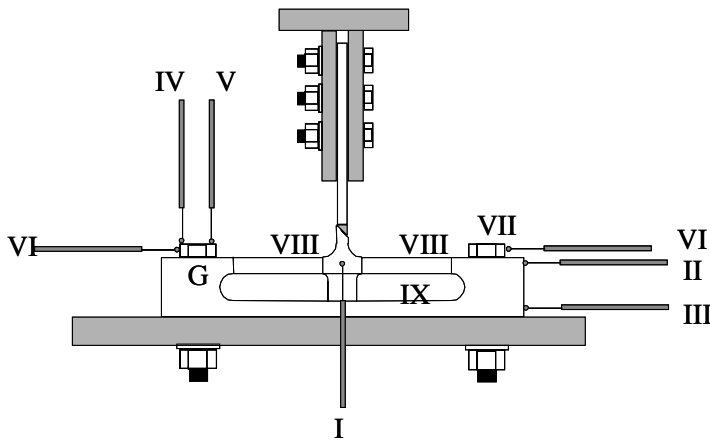


Figure 28. Instrumentation scheme for pilot tests

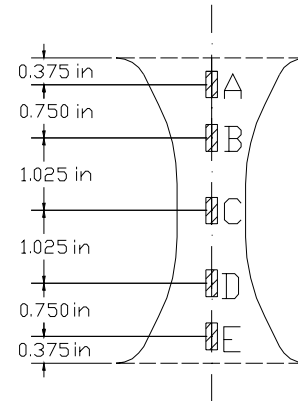


Figure 29. Strain gauge layout on the MC arm.

B. Progress of Modular Node for SMFs

B.1. Introduction

Modular nodes are being developed for use in seismic-resistant steel moment frames. The impetus for developing the modular nodes is the recently discovered susceptibility to fracture of welded-bolted beam-to-column connections in steel special moment-resisting frames (SMFs) during earthquakes. These structures rely on the strength, stiffness and ductility of welded moment connections at the beam-to-column joints to create an efficient lateral-load resisting system (Popov et al, 1989). However, more than 100 SMFs suffered fracture at these welded joints during the Northridge (FEMA-355E, 2000) and Kobe earthquakes (Watanabe et al, 1998). The poor performance of the welded moment connections has raised questions regarding the reliable ductility of the SMFs. It is realized from the research about fully restrained steel moment connections designed following a codified design procedure that a new and effective earthquake-resistant connection design should be based on a combination of weld fracture mitigation measures and changes of connection configuration aimed at reducing the stress levels or redirecting the stress flow in the connection (Stojadinovic and Goel 2000). This paper describes the development of innovative solutions for connecting members in SMFs through a combination of aspects of modular construction and alternative manufacturing processes to provide more reliable and consistent performance of the connections than occurred in the Northridge Earthquake.

The overall objective of this paper is to develop two kinds of new moment resistant connections in two ways: (1) Combine panel zone energy dissipation and modular node concept; (2) Combine beam plastic hinge energy dissipation and modular node concept.

B.1.a Modular Node Concept

The underlying concept in the development of the modular node is the consideration of seismic performance requirements as a first step, prior to establishing the configuration of the connection. The node is then configured directly to meet these requirements. This approach represents a significant departure from current fabrication methods and a major benefit is the ability to remove the field weld from the critical cross-section. The versatility in design required for this approach is

not available under current procedures. Thus, the modular nodes will be created from high-strength high-value steel using a casting process, providing isotropy in material behavior not currently present. While the casting approach renders the modular node viable from a manufacturing standpoint, constructability issues must be addressed.

B.1.b Modular Node Prototype

Two modular node prototypes have been developed: (1) a panel zone (PZ) dissipator; and, (2) a plastic hinge (PH) dissipator. In each case, the modular node is a cast piece that is shop welded to column pieces. Two-tier construction is envisioned in which column assemblages with nodes are erected with beams subsequently field-welded to the modular nodes.

PZ Dissipator: The design intent of the PZ dissipator (See Figure 30) is to provide the majority of seismic energy dissipation through stable yielding of the panel zone. Accordingly, the PZ dissipator employs a weak panel zone relative to the beam, column, and connection region. To accomplish this design, distortion at the beam flange-column flange interfaces and weld location must be mitigated. The following features are included in PZ dissipator design to achieve the objectives: (1) Weak panel zone: dissipates a majority of the seismic energy; (2) Filleted cruciform: helps to reduce the local kinking at beam flange-column flange interface; (3) No web in beam link: it can effectively lower the beam shear by preventing shear reversal between beam flange and beam web and also it gets rid of the problematic region in bolted-web welded-flange connections; (4) Reduced beam link section: yielding outside the panel zone is controlled to occur at this non-critical regions to minimize demands at critical regions for example the weld location; (5)

Flange stiffener: helps to stabilize the beam link flange by reducing secondary bending and kinking at the region close to weld location.

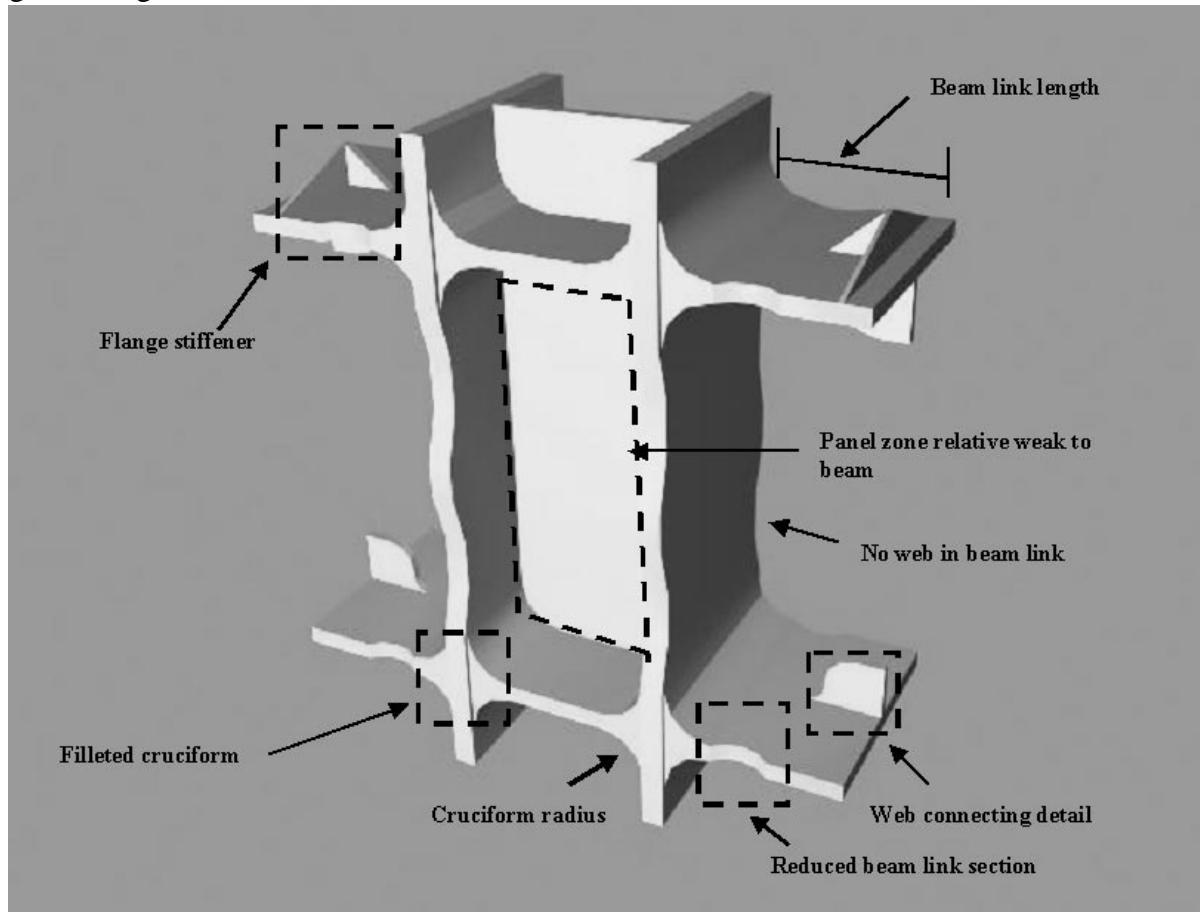


Figure 30. Panel zone dissipator configuration.

The PZ dissipator prototype's final design is completed and prototype specimens are created. Experiment will be ready this week.

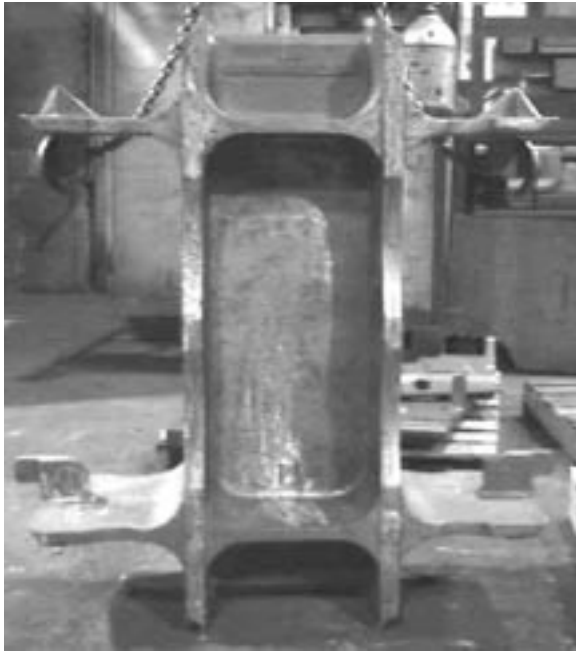


Figure 31. PZ dissipator.



Figure 32. PZ dissipator subassemblage.

PH Dissipator: The PH dissipator has the following important features (See Figure 33): (1) a reduced beam section (RBS) to form a controlled beam plastic hinge region within the node to dissipate a majority of the seismic energy; (2) an isolated web to reduce flange shear; (3) a filleted

cruciform to reduce the column flange kinking; (4) a “balanced” panel zone with respect to the node beam.

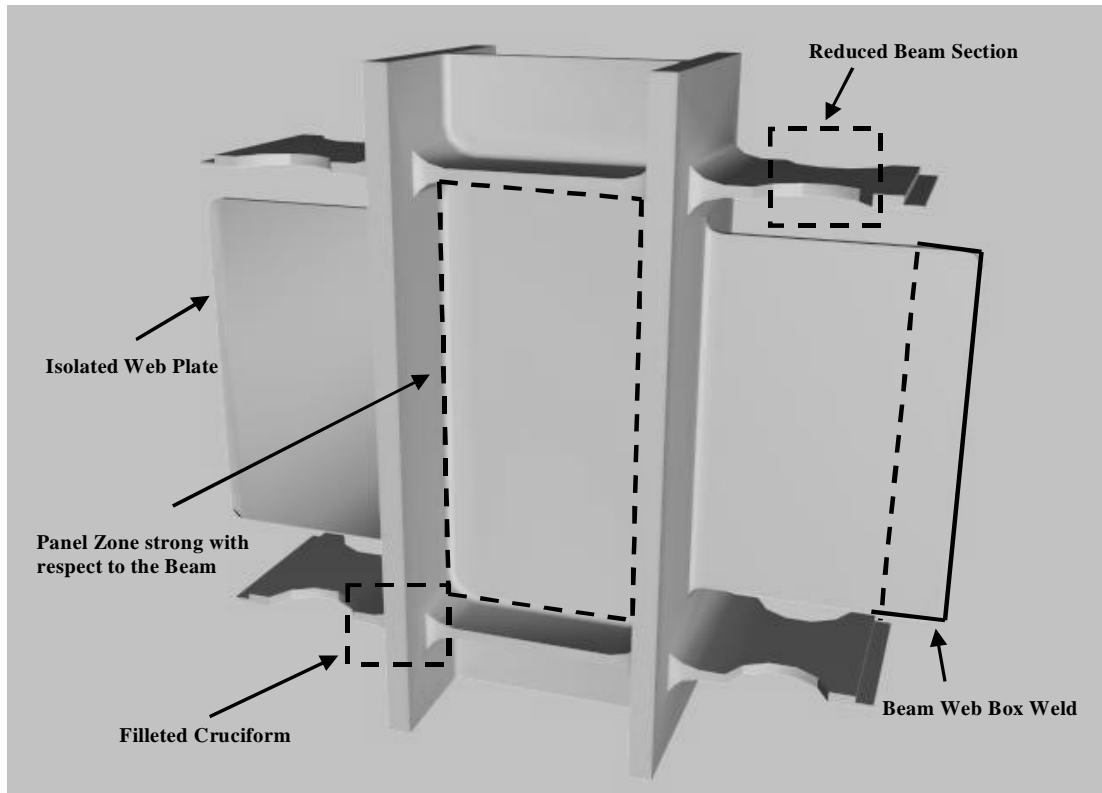


Figure 33. Plastic hinge dissipator configuration.

While the PZ modular node and the PH modular node dissipate energy in quite distinct ways, each of these modular node prototype configurations share two features at the beam flange-column flange interface: (1) Elimination of the field weld; (2) Filletted Cruciform.

(1) Elimination of the Field Weld: The most obvious improvement is the removal of the field weld from the beam-column interface. In the pre/post-Northridge bolted-web welded-flange connections, the field weld requires a weld access hole in the beam flange which creates plastic strain concentrations in the beam. In addition, it is hard to control the quality of weld. Then the flaw of the weld may act as the initiation of crack (FEMA 350). The modular node will greatly reduce the risk of brittle fracture by removing the weld from critical region. A field weld does exist farther from the column face. The stresses at this cross-section are evaluated and minimized.

(2) Filletted Cruciform: Filletted cruciforms occupy the beam flange-column flange interface region in both the PZ and PH modular nodes. The principal reason for these cruciforms in the panel zone is that they can effectively reduce distortion (“kinking”) of the column flange-beam flange intersection during large panel zone plastic shearing. Then the reduction in kinking make it possible for large plastic strain to develop in the panel zone and thus creating a more efficient energy dissipation mechanism than primarily utilizing the beam plastic hinge without high potential in column-beam interface brittle fracture.

In the PH dissipators, the major benefit of the filleted cruciform is the reduction in triaxial tensile stress levels at the column flange-beam flange junction. Additionally, the gradual transition from the beam section to the column section lowers stress concentration due to restraint imposed by the column flange on the beam flange in the transition zone. The filleted cruciform may also brace the RBS for flange lateral buckling.

These features listed above is supposed to effectively reduce the potential for a brittle fracture. The analyze work will be shown later in this paper.

B.2. Background

In the background section, information is provided on related research. Additionally, the node make use of certain details that have been developed. Section 2.A summarizes pertinent research work in the SAC project; Section 2.B describes the reduced beam section (RBS); Section 2.C describes the slotted web connection.

B.2.a SAC Project

The SAC project is a FEMA-sponsored study of steel-frame buildings initiated in the aftermath of the Northridge earthquake. The project was conducted by the SAC Joint Venture: (Structural Engineers Association of California (SEAOC), the Applied Technology Council (ATC) and the California Universities for Research in Earthquake Engineering (CUREe). The aim of the SAC is to address both immediate and long-term needs related to solving performance problems with welded, steel moment-frame connections discovered following the 1994 Northridge earthquake. (FEMA-350) According to the extensive research by SAC, a large number of factors contributed the moment connection failures in the Northridge earthquake. Among these factors, two inherent features played an important role in the susceptibility of connection to brittle fracture: bad local details and poor welding quality (FEMA-350, 2000).

For the welding of beam to column, the detail of weld access holes is produced. Severe strain concentration is created at the toe of these weld access holes due to drastic geometry change. Then the problems like low-cycle fatigue and the initiation of ductile tearing of beam flanges can be caused.

Because of the basic configuration of the welded-bolted beam-to-column connection, it's hard to control and inspect the quality of welding. The poor quality of Northridge welding in enough buildings can not be considered anomaly (FEMA-335E, 2000).

By now, there is no good way to solve these two problems. Increasing the size of the weld access holes can make the welding easier and improve the quality of welding, but it will also increase the brittle fracture potential around weld access holes (El-Tawil, et al., 2000).

t_{cf} = column flange thickness

b_{cf} = column flange width

d_b = depth of the beam

However, it is also realized that significant panel zone yielding can be detrimental to connection performance mainly because the local curvature (“kinking”) of the column at the beam flange-column flange interface provides a high fracture potential at the weld location (El-Tawil 1999, 2000). Thus in order to create a ductile panel zone energy dissipator reducing the effect of kinking to mitigate the possibility of weld fracture will be a top priority for our research.

Under current design provisions, the weak column and strong beam is permitted (UBC 1991, NEHRP 1991). In addition, it is more economical than strong column and weak beam because the beam may be very stiff due to gravity load and serviceability requirement.

Large panel zone deformation may influence the overall behavior of the SMF. Flexible panel zones will reduce the frame stiffness and weak panel zones undergoing large deformation will increase frame drift. It has also been reported that the side-sway stability issues exist under static load (Liew, and Chen 1994). Nevertheless, panel zone deformation is viewed as beneficial to the inelastic dynamic response of the structural system provided certain conditions are met (Schneider 1996).

B.2.c Reduced Beam Section (RBS)

A popular alternative for traditional welded moment connections since the Northridge earthquake has been the RBS connection. The RBS concept is to remove portions of the beam flanges near the beam-to-column connections to make the beam section with reduced flanges to have smaller flexural strength than the beam end. Then the beam plastic hinge zone will move from the beam-to-column interface where the weld is prone to brittle fracture with high plastic demand to the beam. [or The RBS configuration facilitates a ductile plastic hinge in the beam away from the weld through a reduction in the profile of the top and bottom flanges.] Some RBS subassemblies have been tested and enhanced ductility have been shown under cyclic load (Engelhardt, et al. 1996; Chen, et al., 1996; Plumier 1997). The most important dimensions of a RBS are shown in Figure 35. They are: a: the distance from the face of the column to the start of the cut; b: the

length of the cut; c : the lateral depth of the cut. The RBS concept was applied to the PH dissipator modular node.

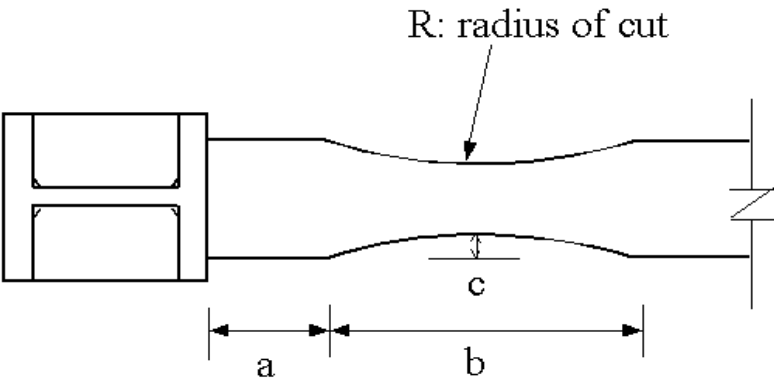


Figure 35. Reduced Beam Section profile.

B.2.d Slotted Web Connection

Slotted web connection is a new type of connection invented by Seismic Structural Design Associates, Inc. (SSDA). It made some modification to the pre-Northridge popular welded-flange bolted-web moment connections by separating the beam flange from the beam web in the region of the connection and welding the web to the column flange. With these changes, the distribution of force and stress and strain are effectively improved. For example, the beam shear sustained by beam flange dropped from 50% of overall beam shear to only 3%. Also the force distribution in the connection are determinate and independent of the interstory drift. Then the Slotted Web Connection has better low cycle fatigue performance compared to both pre-Northridge connection

and RBS connection (Richard, et al. 2001). The basic profile of the Slotted Web Connection is shown in Figure 36.

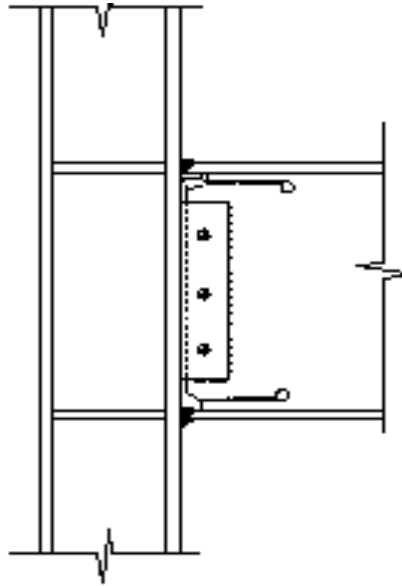


Figure 36. Slotted Web Connection profile.

B.3. Analytical Study

A complex analytical study is conducted to build the modular nodes with good seismic-resistant performance. The characteristics of the analysis subassemblies utilized in the study are derived from a benchmark structure. A nine-story building originally designed as L.A. benchmark structure for the SAC project was chosen as the prototype SMF for the research. The prototype structure was used in order to select realistic modular node designs in both the analytical and experimental evaluation. An interior joint on the first typical floor was selected as the prototype joint. At this joint, W14x193 column frames into a W30x99 beam. The modular nodes are intended for use with any W14 column section. It is envisioned that the modular nodes will be available in a limited set of beam depths.

Table 5: Nominal dimensions for FE subassemblage

Region	Depth (in)	Web Thickness (in)	Flange Width (in)	Flange Thickness (in)
Column (w14x193)	15.48	0.89	15.71	1.44
Beam (w30x99)	29.65	0.52	10.45	0.67
Column (w14x193)	15.48	0.89	15.71	1.44
Beam (w30x173)	30.44	0.66	14.99	1.07

A typical welded-bolted beam-to-column connection which fits the SAC benchmark structure was chosen as the control connection because it is representative of post-Northridge construction practices (See Fig. 3). The behavior and performance of the different configurations of modular nodes are compared to the post-Northridge connections for the purpose of evaluation.

Important geometric parameters are varied to evaluate their effect on behavior. To compare the behavior of the different configurations analyzed in this research and to assess the effect of the parameters of interest, a number of different stress, strain, and combined stress/strain indices are employed.

Analytical modeling was used to evaluate different designs and features of modular node. These models typically encompassed beam-column subassemblage. Two-dimensional and three-dimensional finite element modeling was used.

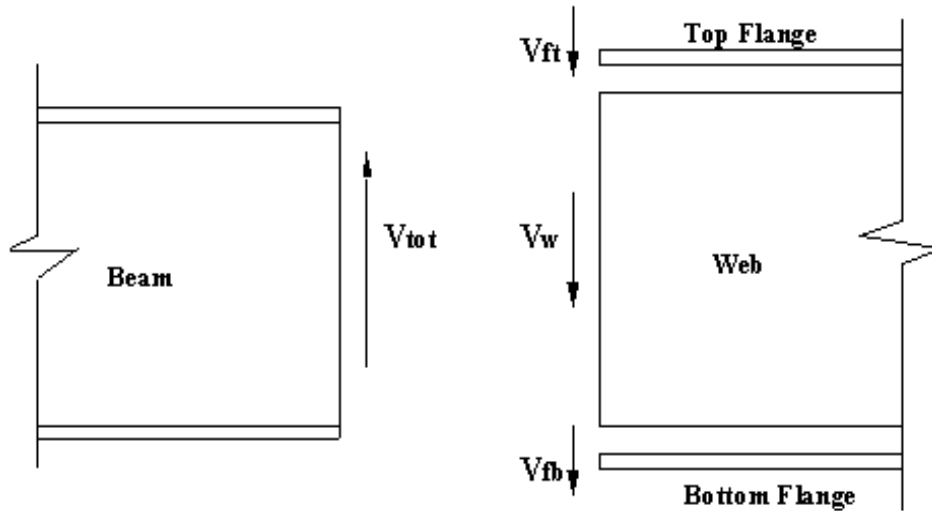
Table 6: Ω_{pz} and corresponding panel zone thickness (2-D)

	SPZ		BPZ	WPZ		
Ω_{pz}	0.5	0.71	1	1.5	2	2.5
t_{pz} A(in)	4.73	3.27	2.26	1.43	1.02	0.78
t_{pz} B(in)	9.13	6.37	4.46	2.90	2.13	1.66

Table 7: Modular Node Parametric Studies

Study	Ω_{pz}	Cruciform Size (in)	Beam Link Length (in)	Special Features
Cruciform Fillet Study	1, 2, 3.76	1, 1.5, 2, 2.5, 3	10	Full, Top, Out, Three fillets
Beam Link Length Study	2, 3.76	3	5.5, 6.5, 7.5, 8.5, 9.5	w/o beam link web
3D study	3.76	1, 1.5, 2, 2.5	11	web tab; no beam link web; w/o beam flange stiffener

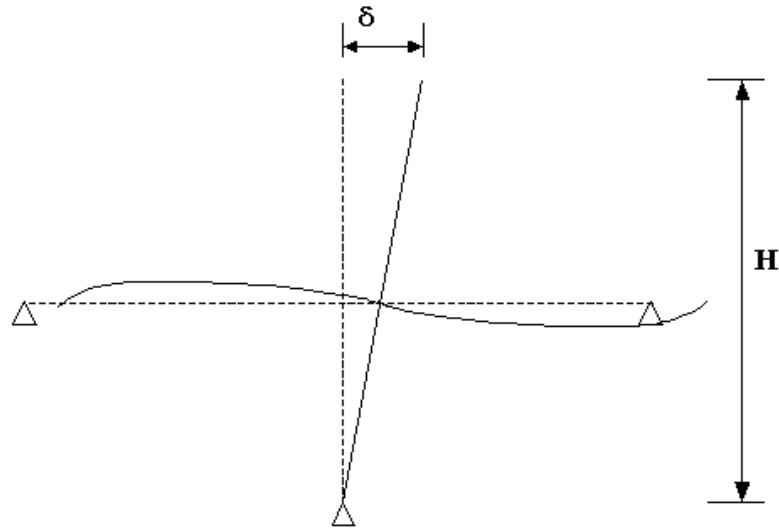
The definitions of beam shear and story drift used in the research are shown in Figure 37 and Figure 38, respectively.



$$\text{Beam Shear Carried by Flange} = (V_{ft} + V_{fb}) / V_{tot}$$

$$\text{Beam Shear Carried by Web} = V_w / V_{tot}$$

Figure 37. Definition of beam shear.



$$\text{Story Drift} = \delta / H \text{ (rad)}$$

Figure 38. Definition of Story Drift.

B.4. Analytical Modeling

Two analytical models were used in the development of modular node: (1) a two-dimensional finite element (2-D FE) model; and, (2) a three-dimensional finite element (3-D FE) model. Due to the intensive computational requirements associated with the 3D-FE model, the 2D-FE model was used to rapidly evaluate parameters and develop the basic form of the modular node configuration. The 3D-FE model was used to verify and fine-tune the 2D-FE model results. Furthermore, because the parametric analyze conducted are for monotonic loading conditions only, it is assumed the conclusions drawn from this research are qualitatively applicable to cyclic loading conditions.

B.4.a Two-dimensional Finite Element (FE) Model

The 2-D FE model is a plane stress representation of a subassemblage in the prototype SMF. The model preserves the projection geometry of the joint in the plane and approximates the correct element stiffness through parametric input of the out-of-plane thickness dimension. While this model possesses limitations in the acquisition of certain data, it was found to be quite potent in rapidly evaluating different configurations accurately with respect to many important measures. In the 2D-FE model, the joint region is modeled with four node (linear) quadrilateral elements. The portions of the beam and column away from the joint are modeled with elastic beam elements. As linear constraint equations cannot be used accurately in a large deflection analysis,

rigid beams are introduced at the free edge of the solid elements to create a plane-section compatibility condition with the interfacing beam element (See Figure 39a, 39b):

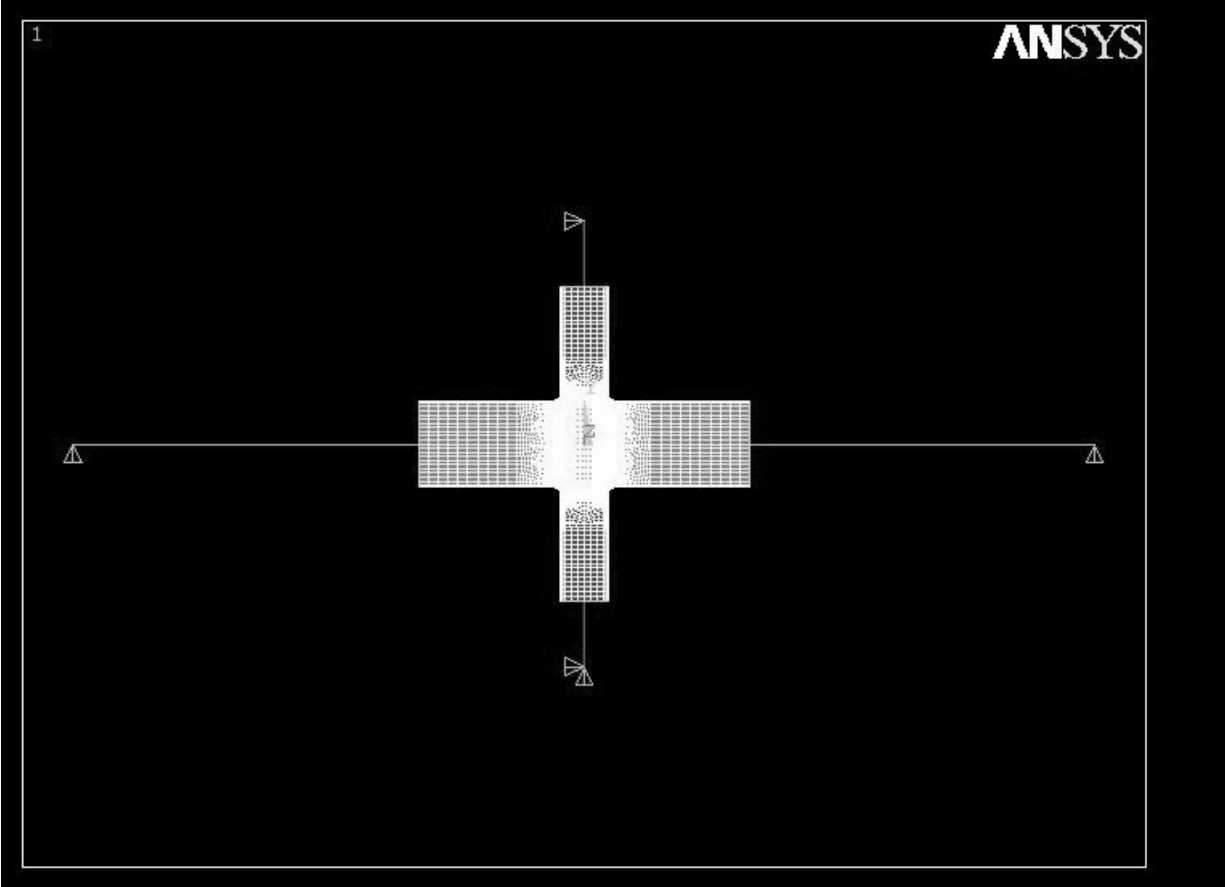


Figure 39a. 2D FE model subassemblage.

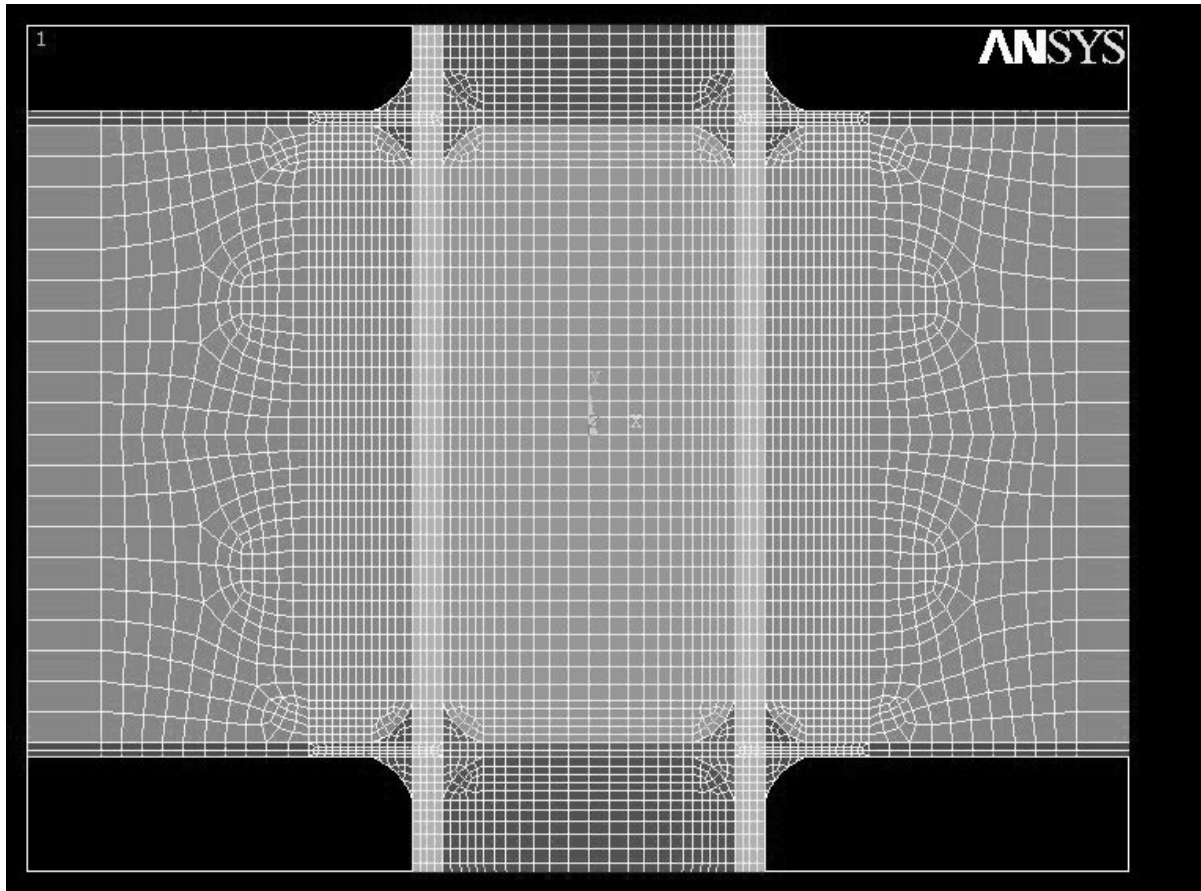


Figure 39b. 2D FE model Panel Zone Detail.

B.4.b Three-Dimensional Finite Element (3D-FE) Model

The 3D-FE model encompasses the same region of the prototype SMF subassembly. Eight-node solid elements are used to model the portions of the beam-to-column joint which undergo inelastic deformation (plastic zone). These elements are transitioned into four-node shell elements for the remainder of the region local to the joint that remains elastic. This region extends a sufficient distance to allow accurate deformation patterns to develop. Only then the plane section compatibility condition is enforced, permitting transition to a line-type beam representation. Elastic beam elements are used to model the outer column and beam regions of the subassembly. At the interfaces of solid elements to shell elements, the multipoint constraint conditions are established to achieve compatibility. Most 3D-FE models developed in this research are half-symmetry about

the plane of the frame. However, a limited number of full 3D-FE models were used to examine torsional stability modes (See Figure 40).

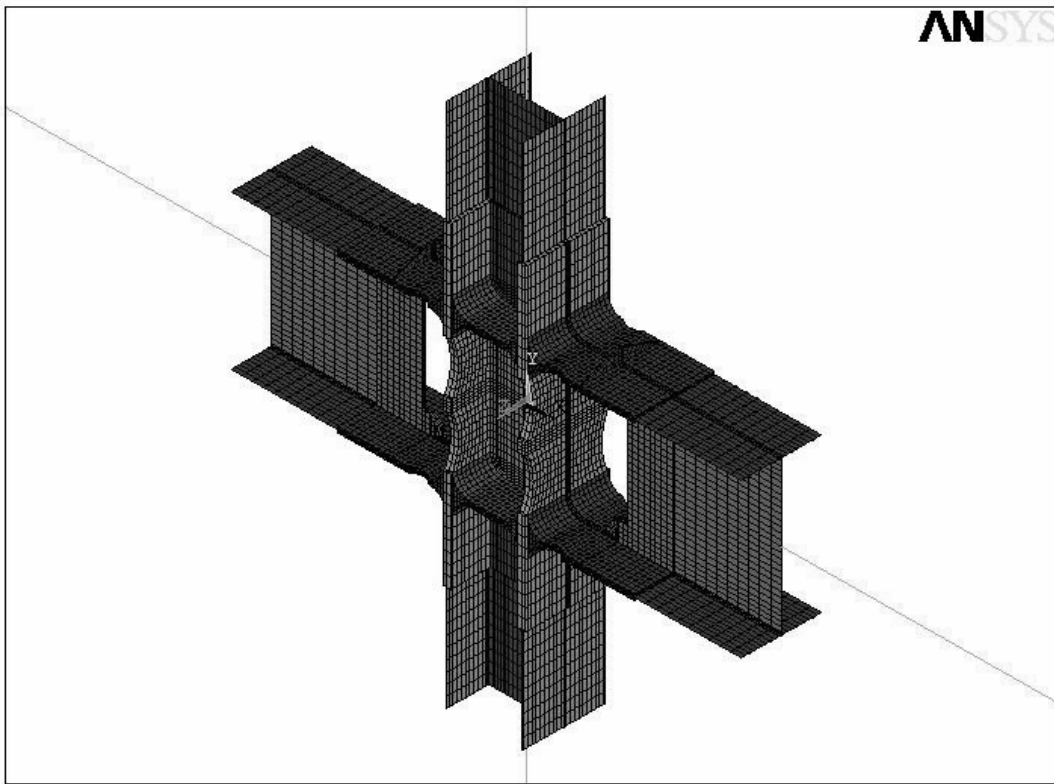


Figure 40. 3D FE model of steel connection subassembly.

B.4.c Validation of 2D Representation

Due to the intensive computational requirement associated with the 3D-FE model, the 2D-FE model was used to evaluate parameters and develop the basic form of the modular node configuration. The 3D-FE model was used to verify the 2D-FE model results. Additionally, the 3D-FE model captures certain behaviors not possible in the 2D-FE model and is used to examine the lateral distribution of some important features. In comparing models of typical configuration, the differences between the models are found to reside within 5% error (see Figure 41, 42). This error was deemed an acceptable level for performing parametric studies to determine the basic configu-

ration of the prototype design of the modular nodes. 3D-FE models are then employed to verify the analysis and to fine tune the final design.

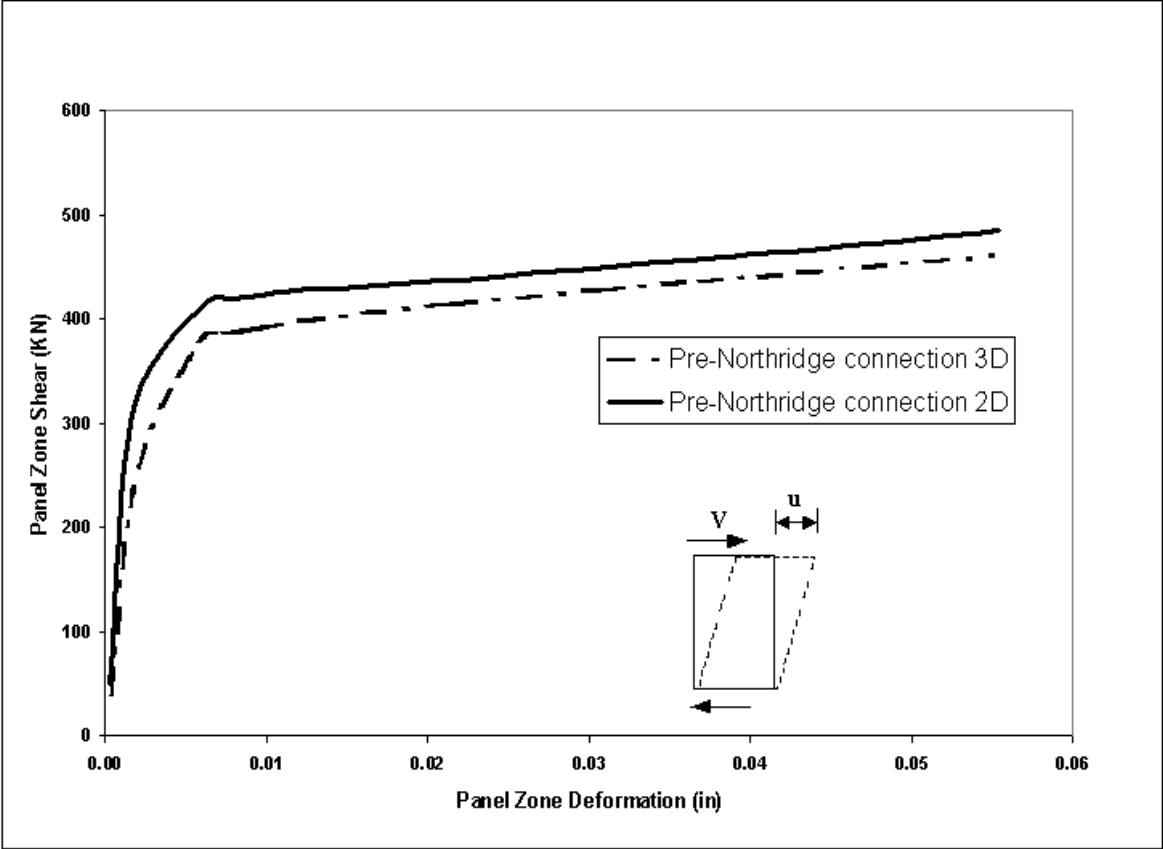


Figure 41. Load-deformation comparison (2D vs. 3D).

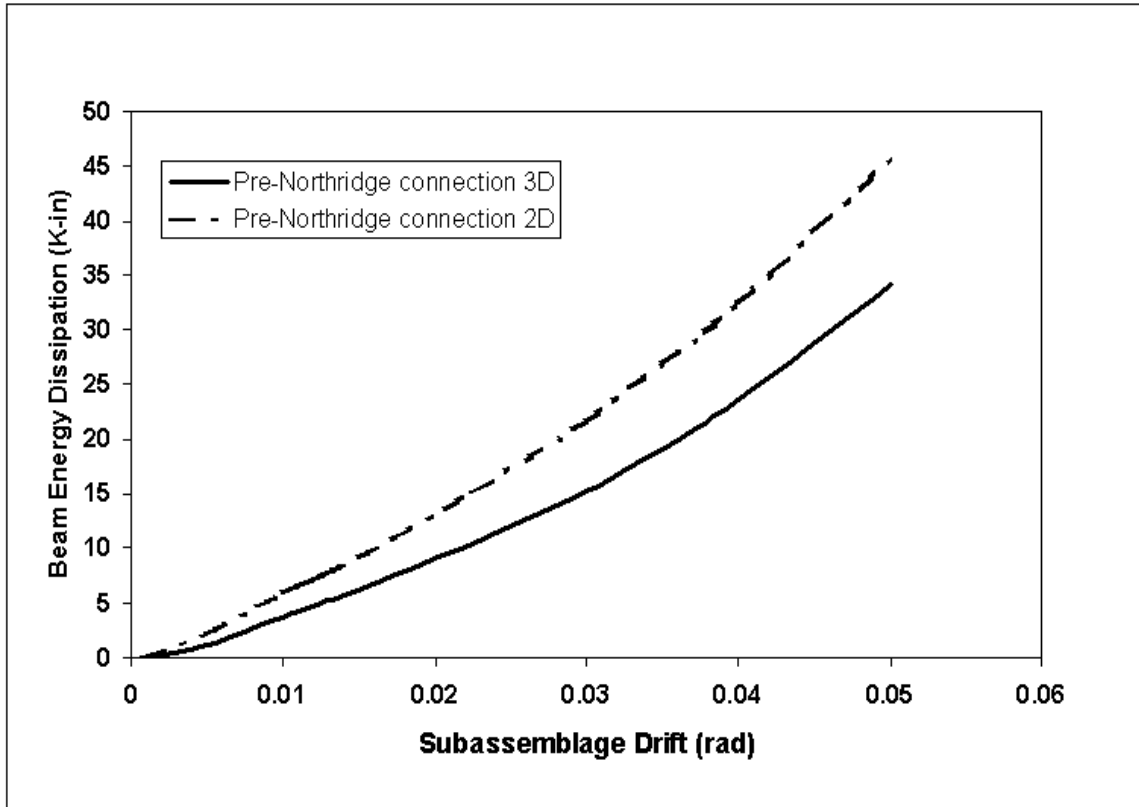


Figure 42. Energy dissipation comparison (2D vs. 3D).

2D-FE Model Mesh Pattern Optimization: In order to minimize the resources consumed by the FE analyze while keeping the accuracy of results, a 2D-FE model mesh pattern study was performed to get good and economical mesh pattern. As a result, the Fine Mesh was found to be acceptable for our 2D FE subassembly. Figure 43 shows the comparison for results from Coarse Mesh, Fine Mesh and Very Fine Mesh:

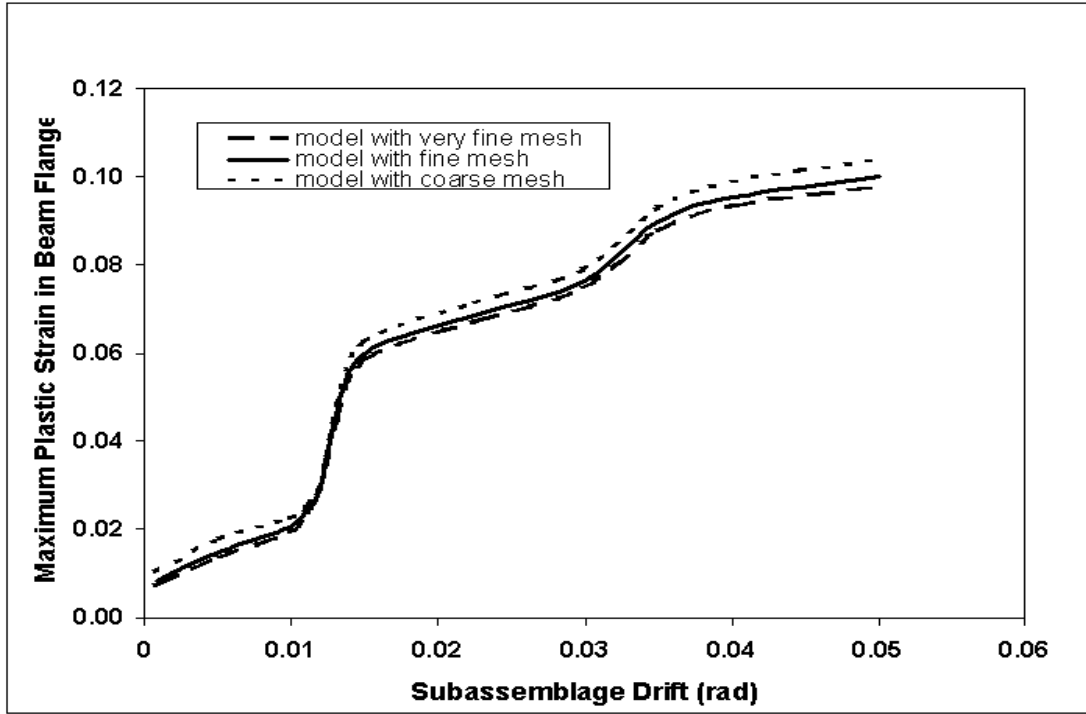


Figure 43. Strain results comparison for different mesh patterns.

B.5. Performance indicators

The following measures were used to evaluate the modular node and compare performance with the post-Northridge moment connection (traditional connection).

(1) Triaxiality: High triaxial stress can suppress yielding thus inducing ductile metals to perform in a brittle manner (Schafer et al. 1999). The highly restrained region at the column flange-beam flange junction renders triaxiality an important index for moment connections. Triaxiality has been cited as a potential cause of the poor performance of the moment connections in the 1994 Northridge earthquake (Yang and Popov 1995; SAC 1996). Triaxiality is defined here as the ratio of the principal stress at a point to the deviatoric stress that causes yielding.

$$T_2 = \frac{\sigma_1}{\sigma_{eff}}$$

$$\sigma_{eff} = \sqrt{\frac{1}{2} \sqrt{(\sigma_1 \ominus \sigma_2)^2 + (\sigma_2 \ominus \sigma_3)^2 + (\sigma_1 \ominus \sigma_3)^2}}$$

where σ_i , $i=1, 2$, and 3 , are the principal stresses at a point. Investigation employing a triaxiality fracture criterion applied to moment connections indicate that brittle behavior of these connections may be governed by triaxiality even when high toughness metals are used.

(2) Panel Zone Energy dissipation: the energy dissipated by panel zone: It is calculated by:

$$E_{pz} = \int F_{pz} d\delta$$

where δ is the panel zone deformation; F_{pz} is the panel zone shear force.

(3) Plastic Hinge Energy dissipation: the energy dissipated by plastic hinge. It is computed by:

$$E_{PH} = \int M_{beam} d\theta_{pl}$$

where θ_{pl} is the beam plastic rotation; M_{beam} is the beam moment.

(4) Column flange curvature: the kinking at column flange, as shown calculated in Figure 44:

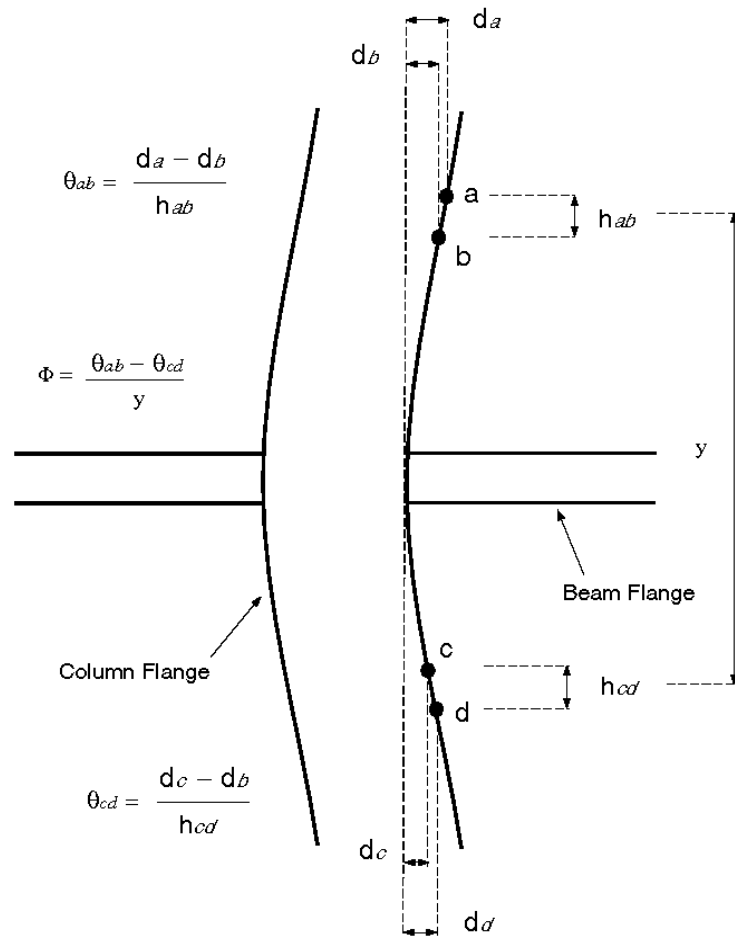


Figure 44. Measurement of kinking.

(5) Beam shear distribution: the ratio of the shear carried by the beam link flange to the total shear carried by the beam link.

(6) PZ shear development: the increase of PZ shear with the deformation of PZ.

(7) Maximum plastic strain in local regions: Maximum equivalent plastic strain was measured at the following regions of the node: panel zone, column flange and beam link.

B.6. Parameters

Most of the modular node connection configurations were varied for evaluation by changing the following three important parameters in the research: (1) beam to PZ relative strength Ω ; (2) filleted cruciform size R; (3) beam link length L.

(1) Beam to Panel Zone Strength Ω : An important measure used to characterize the connections is the relative strength of the beam plastic hinge zone to the panel zone. A panel zone overstrength index, Ω is established to express this relation. Ω is defined as the ratio of the total equivalent flange force translated to the continuity plates at the development of the beam plastic moment to the nominal shear capacity of the panel zone:

$$\Omega = \frac{2F}{V_{pz}} = \frac{\frac{2M_p}{d_b}}{V_{pz}}$$

The energy dissipation percentage by panel zone and beam plastic hinge will be apparently affected by Ω . The nominal strength of the beam end and the PZ are equal when Ω is unity. Thus, a balance of dissipated energy would be anticipated for such a design. In the paper, $\Omega < 1$ will be termed a ‘Strong Panel Zone’ (SPZ) design and $\Omega > 1$ will be termed a ‘Weak Panel Zone’ (WPZ) design. Ω for this study was adjusted by changing the thickness of the panel zone.

(2) Filleted Cruciform Size: The radius of the fillet curves are used to measure the filleted cruciform (See Figure 45). It is a very important geometry to reduce the local kinking at the column flange-beam flange interface.

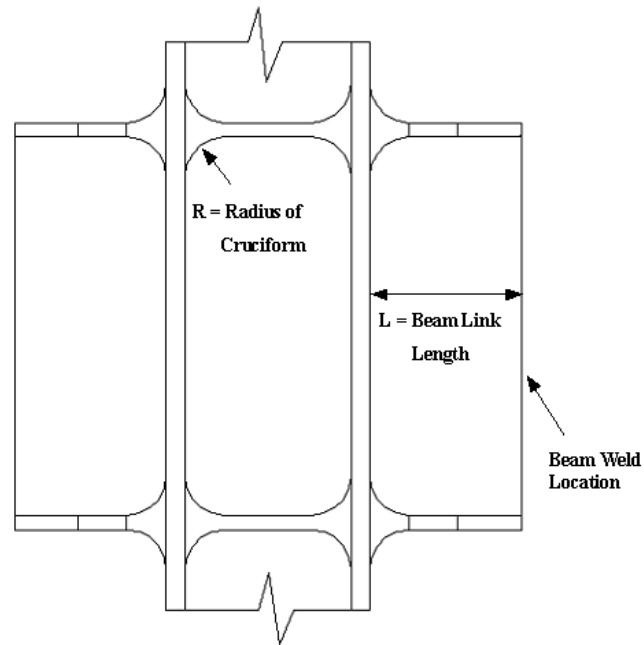


Figure 45. Schematic plot of a simple modular node connection.

(3) Beam Link Length: The beam link is the modular node beam region (See Figure 45). It is a very important geometry in developing beam plastic hinge and reducing kinking at the beam weld location.